2007-07-13

A Geometry-Based Motion Planner for Direct Machining and Control

Robert M. Cheatham
Brigham Young University - Provo

A GEOMETRY-BASED MOTION PLANNER FOR DIRECT MACHINING AND CONTROL

by

Robert Marshall Cheatham

A thesis submitted to the faculty of

Brigham Young University

in partial fulfillment of the requirements for the degree of

Master of Science

Department of Mechanical Engineering

Brigham Young University

August 2007

BRIGHAM YOUNG UNIVERSITY

GRADUATE COMMITTEE APPROVAL

of a thesis submitted by

Robert Marshall Cheatham

This thesis has been read by each member of the following graduate committee and by majority vote has been found to be satisfactory.

Date	C. Gregory Jensen, Chair
Date	W. Edward Red
Date	Thomas W. Sederberg

BRIGHAM YOUNG UNIVERSITY

As chair of the candidate's graduate committee, I have read the thesis of Robert Marshall Cheatham in its final form and have found that (1) its format, citations, and bibliographical style are consistent and acceptable and fulfill university and department style requirements; (2) its illustrative materials including figures, tables, and charts are in place; and (3) the final manuscript is satisfactory to the graduate committee and is ready for submission to the university library.

Date

C. Gregory Jensen
Chair, Graduate Committee

Accepted for the Department

Matthew R. Jones
Graduate Coordinator

Accepted for the College

Alan R. Parkinson
Dean, Ira A. Fulton College of
Engineering and Technology

ABSTRACT

A GEOMETRY-BASED MOTION PLANNER FOR

DIRECT MACHINING AND CONTROL

Robert Marshall Cheatham

Department of Mechanical Engineering

Master of Science

Direct Machining And Control (DMAC) is a new method of controlling machine tools directly from process planning software. A motion planning module is developed for the DMAC system that operates directly off path geometry without pre-tessellation. The motion planner is developed with the intent to process Bezier curves. The motion planning module includes a deterministic predictor-corrector-type curve interpolator, a dynamics limiting module, and a two-pass jerk-limited speed profiling algorithm. The methods are verified by machining an automotive surface in a clay medium and evaluating the resultant machine dynamics, feed rate, and chordal error throughout the machining process.

ACKNOWLEDGMENTS

I would like to thank my thesis committee for their helpful advice and encouragement. Specifically, Dr. Greg Jensen for bringing me into such an interesting area of research, Dr. Ed Red for his happy demeanor and for sharing his knowledge of speed profiling and dynamics, Dr. Thomas Sederberg for introducing me to the exciting field of computer-aided geometry, and all three of them for their supererogatorily positive attitudes and unmatched enthusiasm for their fields of research. I appreciate it more than they know.

I also want to thank my parents for their love, strength, and support; for providing me with a life foundation upon which I could build a successful educational experience; and for never letting me slack off during the formative years. All of which gave me the boost I needed, and helped turn a dreamy kid into a pretty good engineer.

TABLE OF CONTENTS

LIST OF TABLES

LIST OF FIGURES

NOMENCLATURE

$\lvert\cdot\rvert$	Absolute value of a variable or vector
$\lVert\cdot\rVert$	Magnitude of a vector
a	Beginning of a parameter interval
A	Acceleration
A_d	Desired acceleration
A_{end}	Acceleration at the end of a speed profile segment
A_{start}	Acceleration at the beginning of a speed profile segment
$A(t)$	Acceleration as a function of time
A_{max}	Maximum attained acceleration value for a speed profile segment
A_r	Radial acceleration
b	End of a parameter interval
$B_i^n(u)$	Bernstein polynomial
d	Endpoint derivative of a Sarfraz curve – reciprocal of the magnitude of the tangent vector of the associated parametric curve
$\Delta A_{concave}$	Change in acceleration over a concave speed profile segment
ΔA_{convex}	Change in acceleration over a convex speed profile segment
$\Delta S_{concave}$	Distance traveled over a concave speed profile segment
ΔS_{convex}	Distance traveled over a convex speed profile segment

ΔS_{fall}	Distance traveled over the fall portion of a speed profile
ΔS_{rise}	Distance traveled over the rise portion of a speed profile
$\Delta t_{concave}$	Time to complete a concave speed profile segment
Δt_{convex}	Time to complete a convex speed profile segment
$\Delta V_{concave}$	Speed change over a concave speed profile segment
ΔV_{convex}	Speed change over a convex speed profile segment
ΔV_{rise}	Total speed change over the rise portion of a speed profile
Δu	Parameter interval
ε_{length}	Maximum allowable length error due to selection of parameter u
$\varepsilon(S', n, a, b)$	Error function of Gauss-Legendre quadrature
$f^{(i)}(u)$	ith parametric derivative of a function f
$f'(u)$	First parametric derivative of a function f
$f''(u)$	Second parametric derivative of a function f
$f'''(u)$	Third parametric derivative of a function f
$f_S(u)$	First derivative of a parametric function f with respect to arc length
$f_{SS}(u)$	Second derivative of a parametric function f with respect to arc length
$f_{SSS}(u)$	Third derivative of a parametric function f with respect to arc length
$\dot{f}(u)$	First derivative of a parametric function f with respect to time
$\ddot{f}(u)$	Second derivative of a parametric function f with respect to time
$\dddot{f}(u)$	Third derivative of a parametric function f with respect to time
ϕ	Angular dimension in a cylindrical coordinate system

i	An index
j	An index
J	Jerk
J_0	Jerk value specified for a speed profile segment
J_{max}	Maximum allowable jerk value for a speed profile segment
$J(t)$	Jerk as a function of time
k	An index
$\mathbf{K}$	Inverse kinematics transformation
K_n	Degree-dependent constant in Gauss-Legendre quadrature error function
l	An index
L	Linear travel on the axis of a machine tool
m	Number of independent machine joints
$\max[f]$	Maximum value of a function f
$\max[\mathbf{f}]$	Maximum value of the components of a vector **f**
$\min[\mathbf{f}]$	Minimum value of the components of a vector **f**
n	Degree of a parametric curve
N_{table}	Number of divisions in parameter-length lookup table
$\mathbf{P}$	A point in 3D Cartesian space
P_x	x-component of a 3D Cartesian point
P_y	y-component of a 3D Cartesian point
P_z	z-component of a 3D Cartesian point
$\mathbf{P}(u)$	A parametric curve in 3D Cartesian space
$q_i(\mathbf{P})$	Position of i^{th} joint as a function of point **P**

$\mathbf{q}(u)$	A parametric curve in m-dimensional joint space
$\mathbf{q}^m$	An m-dimensional joint space
θ	Normalized parameter value for Sarfraz curve
r	Radial dimension in a cylindrical coordinate system
R	Radius of curvature
S	Desired length along a parametric curve
S_L	Length of a line
S_P	Length required to traverse a speed profile
S_{start}	Distance traveled at the beginning of a speed profile segment
$S(t)$	Length as a function of time
$S(u)$	Length along a parametric curve as a function of the parameter
$S'(u)$	Parametric speed along a parametric curve. Also the magnitude of the tangent vector of a parametric curve.
t	Time
T	Time to complete a perfect s-curve speed profile
u	Parameter of a parametric curve
$\dot{u}$	Time rate of change of the parameter of a parametric curve
$u(S)$	Sarfraz curve –parameter as a function of length along a parametric curve
v	Weighting value in a Bezier curve
V	Velocity
V_d	Desired velocity
V_{start}	Velocity at the beginning of a speed profile segment
$V(t)$	Velocity as a function of time

w	Tabulated weighting value used in Gauss-Legendre quadrature.
ω	Weighting value in a Sarfraz curve
x	Tabulated constant used in Gauss-Legendre quadrature, 1st dimension in a rectangular coordinate system
y	2nd dimension in a rectangular coordinate system
z	3rd dimension in a rectangular coordinate system, linear dimension in a cylindrical coordinate system

1 INTRODUCTION

1.1 DIRECT MACHINING AND CONTROL

Direct Machining And Control (DMAC) is a new method of controlling machine tools [1, 20]. Developed at Brigham Young University, DMAC is designed to make manufacturing processes CAD-centric as opposed to the current ASCII-based, M&G code-centric process. The DMAC concept provides for an open-architecture PC software controller. One of the unique differences between DMAC and traditional machine control is that the process planning software (CAD/CAM systems, robotic simulation software, coordinate measuring software, process optimization software, etc.) resides on the same computer as the machine control software.

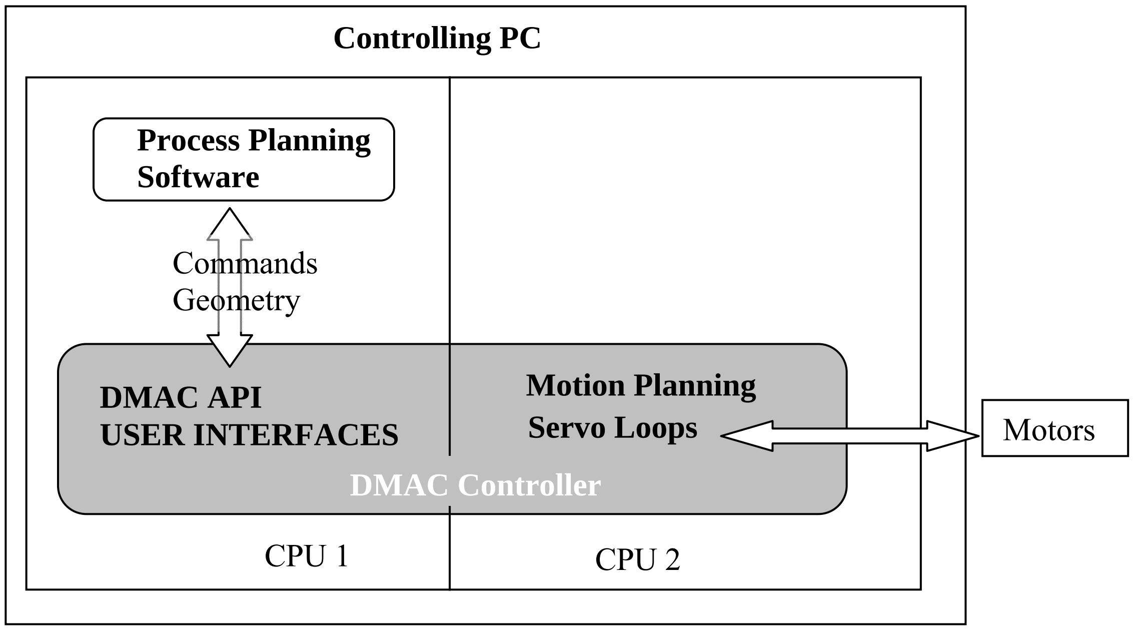

Figure 1.1. DMAC Architecture

The DMAC controller consists of a dual processor or dual core computer running two operating systems, currently Windows XP and Ardence RTX. One processor runs Windows and the process planning software while the other runs RTX and the DMAC control software (Fig. 1.1). Running these two operating systems simultaneously is necessary because the most common process planning software packages support the Windows operating system, but Windows does not provide a real time control capability. This is provided by RTX, where the control portion of DMAC is housed. These operating systems are linked by shared memory. Thus the process planning software can be linked directly to the machine tool. Information in the form of tool paths, I/O commands, machine states, and sensor readings are passed between the process planning software and the controller via function calls and shared memory. This gives real time decision-making capability to process planning and factory control software so that changes can be made at the process plan level while the job is in-process. Also, since manufacturing operations are controlled directly from the process plan there is no disassociation from the original part file. No translation is necessary so the data remains in its native format and no error is introduced.

This is in contrast to the current industry standard of M&G code, as illustrated in Fig. 1.2. Controllers adhering to M&G code standards accept process steps and sequences in the form of ASCII block-formatted commands. These process steps consist of mechanism commands, such as speed, coolant flow, and tool changes, and movement commands that consist of tessellated geometry – line segments and arcs. The tessellated moves require blending to achieve smooth motion. For contouring operations in particular, some controllers refit the tessellated tool paths with splines as a preprocessing operation.

A weakness in this methodology is that once the ASCII files are generated, they are no longer associated with the original process plan. No information or changes can flow to or from the original process plan without regeneration of the ASCII file or manual intervention. This is strictly a unidirectional data flow. Another weakness is that the tessellated geometry does not reflect the native geometric data in the process plan, since many process planning systems store their tool paths as splines such as NURBS. Upon postprocess, these splines are tessellated to work with the M&G code standard. The refitting of tessellated moves by the controller (discussed above) introduces error and further disassociates the manufacturing operation from the original CAD model and process plan.

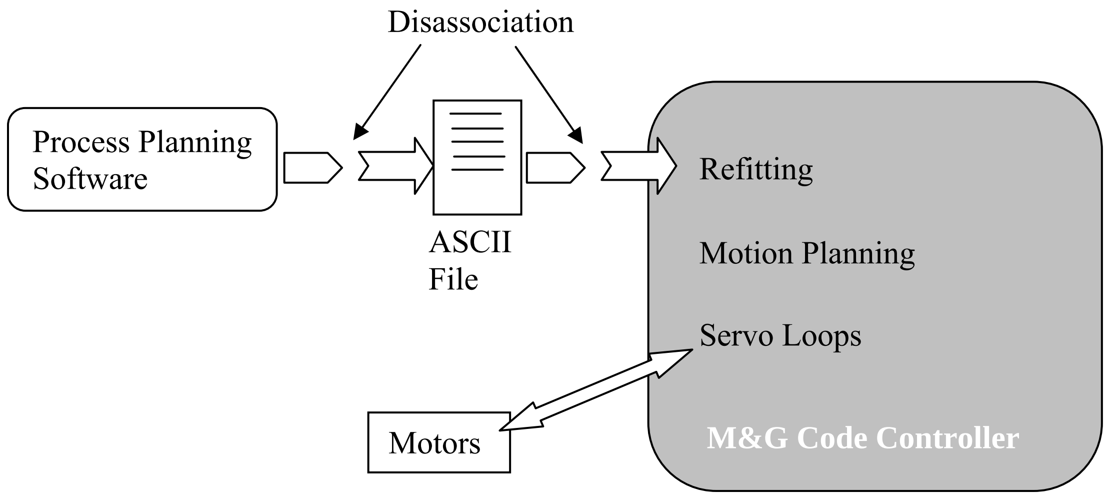

Figure 1.2. M&G code architecture.

Direct Control uses the native process geometry (splines, lines, arcs, etc.). This maintains the original manufacturing intent and also gives the process planning system an additional degree of control over the machine motion. Many spline generation methods have been developed for achieving smooth motion, but Direct Control allows the process planning software to choose a spline generation method that is best suited to the application.

1.2 THESIS TOPIC

A typical machine controller architecture is shown in Fig. 1.3. Path geometry is input into the controller, which is then pre-processed and fed into the motion planner. The motion planner generates position commands and feeds them to the servo controller, which generates the proper commands for the amplifiers and motors.

This thesis will develop a working parametric curve module for the DMAC controller's motion planner. Specifically, this module will be applicable to parametric polynomial curves such as Bezier and NURBS curves. The philosophy behind Direct Machining is to use the actual geometry provided by the process planning software. Therefore the parametric curve module will be completely geometry-based, meaning there is no pre-tessellation of the curves into linear segments.

1.2.1 BEZIER-BASED APPROACH

NURBS curves are the dominant curve definition used in today's CAD/CAM systems. However, Bezier curves offer cleaner algebraic expressions and simpler algorithms than

NURBS curves. This thesis will therefore develop algorithms with reference to Bezier curves. Little is lost in this approach since algorithms for Bezier curves can be generalized for NURBS by readers experienced in computer-aided geometry.

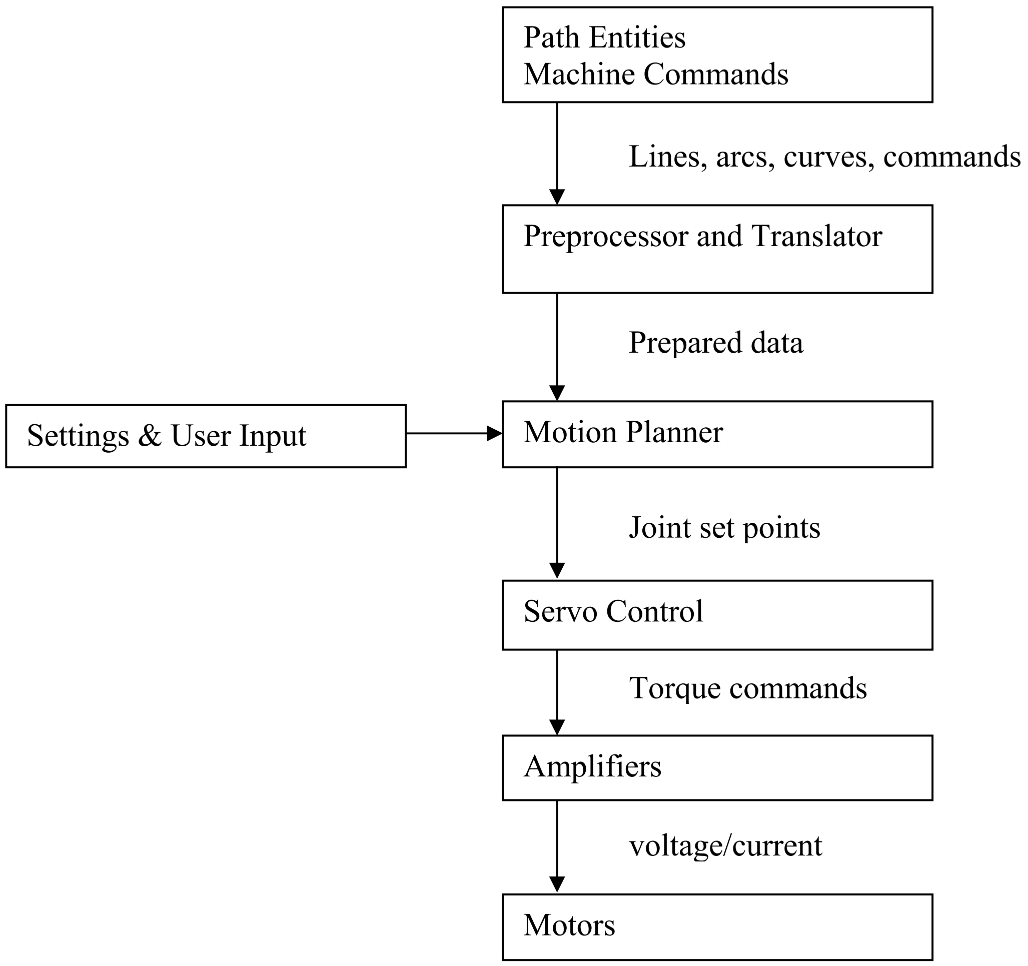

Figure 1.3. Typical controller architecture.

1.3 CONTRIBUTIONS

Traditional control methods rely on pre-tessellation of the data, where the original geometric entities are discarded after being digitized into a set of points. This tessellated data is then loaded into large buffers known as look-ahead buffers, and the motion planned over the tessellated points. This thesis will explore the nuances of planning motion *directly* on path geometry and will present methods to solve the associated problems.

Currently no papers deal satisfactorily with operating directly on parametric path geometry. A complete method is necessary to account for the complexities that develop due to interactions between the various elements in a motion planner including speed profiles, dynamics, path accuracy, and accurate feed rate. Most path-following papers deal with only one of these aspects individually, and nearly all ignore motion dynamics. This thesis will develop methods for path-following that integrate all necessary elements of a motion planner, comprised of 3 main parts:

1) A stable predictor-corrector for selecting the appropriate evaluation point of the curve. This is necessary due to the difficulty of predicting the parameter associated with a specific length along a parametric curve. Current algorithms in the literature can have low convergence rates and are mainly extrapolative. These extrapolations are inherently unstable and can cause errors in the prediction process unless additional constraints or stable correction methods are used. Fig. 1.4 illustrates this, where the use of Lagrange interpolation to generate a prediction curve yields a decreasing region. The predictor-corrector will be verified by plotting the feed rate errors for motion along a process plan.

2) A reliable and accurate speed profiler to maintain controlled motion. This is necessary because current algorithms only consider a simple speed profile over a single move and do not account for dynamics. With current methods, situations quickly develop where a feasible speed profile cannot be generated. Fig. 1.5 illustrates this condition, where the third profile segment cannot decrease speed enough to reach the allowable speed for the following segment. The speed profiler will be verified by plotting the tool speed along a process plan along with the desired and allowable speeds.

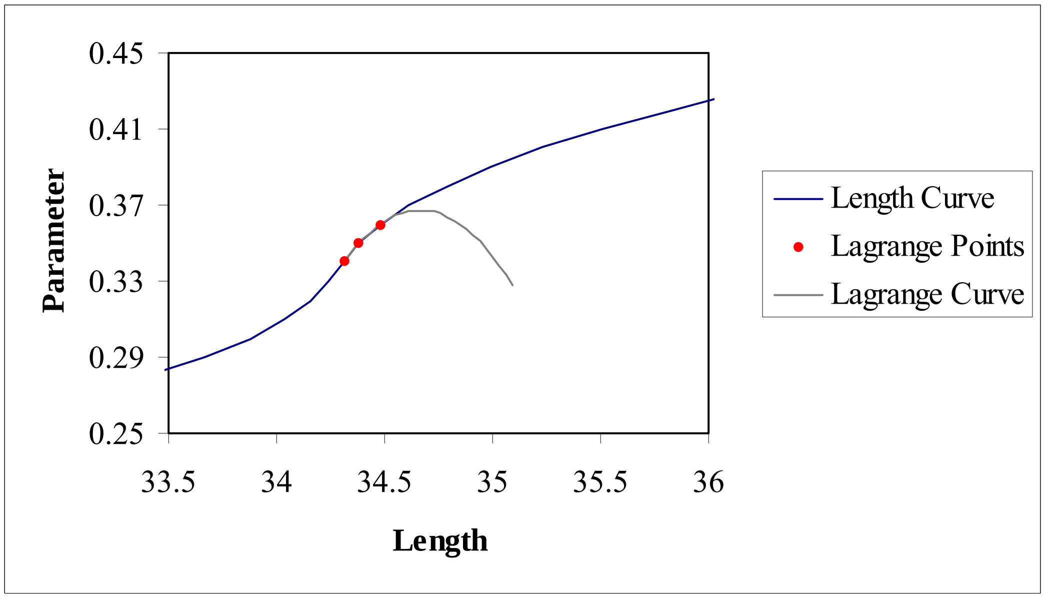

Figure 1.4. Extrapolative prediction method doubling back on itself.

3) An approach to motion dynamics and path accuracy that keeps the speed, acceleration, and jerk of machine axes within set limits. This will be verified by plotting the machine dynamics and chordal error along a process plan.

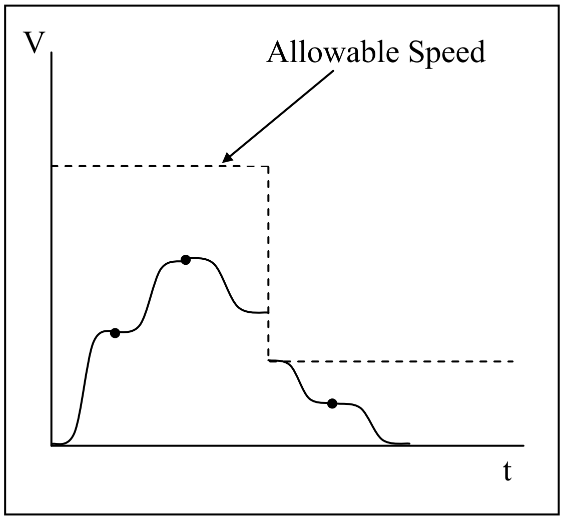

Figure 1.5. Infeasible speed profile caused by violation of allowable speed.

1.4 DELIMITATIONS

This thesis will focus on 3-axis milling; 5-axis methods will not be considered. Also, the thesis will follow the provided paths, meaning that no methods will be devoted to curve generation, path smoothing, or blending between paths.

Since this thesis explores new subject matter, the focus will be on finding stable methods that work and are reasonably fast. The development of more advanced methods will be left to future research.

1.5 VERIFICATION OF METHODS

An automotive body panel will be 3-axis machined in a clay medium on BYU's Tarus styling mill. Since the motion waypoints will always be located exactly on the tool paths, the motion is assumed to be accurate. The main concern is maintaining speed and respecting motion dynamics. Therefore, this panel will only be visually inspected for surface quality. During the machining process, data will be collected concerning the feed rate error, tool speed, machine dynamics, and chordal error. The three main portions of the path following methods will be verified by:

1) Inspecting the results for the feed rate error. If these results are within the allowable feed rate error, the predictor-corrector method is acceptable.

2) Inspecting the tool speed, machine dynamics, and chordal error for the process plan. If the tool speeds do not violate the allowable speeds and hold the desired speed well, the machine dynamics are kept within bounds, and the chordal error is kept within the machining tolerance, then the speed profiling and motion dynamics methods are acceptable.

2 BACKGROUND

The first computer-controlled (Numerically Controlled or NC) machine tool came online in 1952 at the MIT Servomechanisms Laboratory. This machine was the result of a project commissioned by the Parsons Aircraft Company and supported and funded as a US Air Force project. This machine was the fulfillment of a need for a machine control system that could manufacture the increasingly complex parts used in aircraft.

This first machine controller accepted command inputs from punched tape. These commands were discrete machine commands such as “spindle on.” Motion commands were simple “goto” commands. The servo algorithms were simple chaser algorithms that attempted to move the servo motors to the next point.

Since there were no algorithms to slow the machine, this would result in overshoot after the machine reached the desired point, and the machine would oscillate as the controller attempted to settle onto the point. This effect could be minimized by breaking long lines into shorter segments and specifying decreasing speeds near the end of the movement [25]. However, this process was time-consuming and increased the size of part programs resulting in greater data storage and processing needs.

Motion planning modules were developed to remove the burden of ensuring proper acceleration and deceleration from the part program and place it on the controller. This was again accomplished by breaking long lines into shorter segments, but motion planners accomplished this online and at much finer resolutions. Motion planners also enabled the controller to process curves such as conics and parametric curves.

By the early 1970's, NC machines had been combined with microprocessor technology to form Computer Numerically Controlled (CNC) machines. These new controllers could read in an entire part program and store it in memory [16]. This allowed for faster execution of the program, yielding higher feed rates and better accuracy. CNC machines also had simple motion planners, resulting in better feed rate control and better control of overshoot.

These first motion planners were simple, consisting of interpolators and basic acceleration/deceleration algorithms. Interpolators discretized the moves to yield specific positions for the motors to go to. The accel/decel algorithms helped to regulate forces on the motors and power transmission assemblies [16].

The remainder of this chapter describes the historical development of motion planning algorithms. Section 2.1 explains the development of curve interpolation methods. Section 2.2 follows the development of speed control methods. Section 2.3 describes the methods for limiting basic motion dynamics.

2.1 CURVE INTERPOLATION

NC and CNC machine controllers are digital. This means that the motors are controlled at finite time intervals. Waypoints are provided by the motion planner's interpolation module to the servo controller at a specified frequency. The frequency, position, and spacing of these waypoints determine the motion and speed of the machine. Correct spacing of the waypoints along a path is critical for maintaining path accuracy, proper tool speed, and acceptable machine dynamics.

Section 2.1.1 explains the two basic types of interpolation modules. Section 2.1.2 follows the development of interpolation techniques for parametric curves.

2.1.1 THE TWO TYPES OF CURVE INTERPOLATORS

In machining control methods, there are two main types of curve interpolators: reference-pulse interpolators and reference-word (also referred to as sampled-data) interpolators. To understand these, the concept of a basic-length unit (BLU) must be explained. BLU refers to the resolution of the controller for an individual axis. For a controller with n bits of resolution and an axis travel L, the BLU is

$$\mathrm{BLU} = \frac{L}{2^n} \tag{2.1}$$

Reference-pulse interpolators work on a timed clock cycle. For every cycle of the interpolator, the output for each axis is either a one or a zero. If the output is a zero, the axis is held steady. If the output is a one, the axis is incremented by one BLU. Reference-pulse interpolators are usually used in open-loop control (no feedback) in concert with stepper motors. Since reference-pulse interpolators can only increment the axis by one BLU per cycle, the maximum speed an axis can be moved is

$$V_{max} = f \cdot BLU \tag{2.2}$$

where f is the frequency at which the interpolator is executed [16]. The most commonly used reference-pulse interpolator is the digital differential analyzer (DDA) due to its ability to hold uniform velocity around a circular arc [17].

Reference-word interpolators, such as the Tustin Method for circular arcs [16], are able to hold higher speeds due to the fact that they can generate a target at any point along a path. This effectively allows them to specify motion at any velocity. Whereas the velocity of machines controlled with reference-pulse interpolators is typically controller-limited, the velocity of machines controlled with reference-word interpolators is limited by the capabilities of the motors and transmission systems on the machine. Reference-word-type interpolators are used for today's parametric curve interpolation modules.

2.1.2 PARAMETRIC INTERPOLATORS

With Bezier curves, the difficulty lies in reconciling the highly nonlinear relationship (see Farouki [10]) between the parameter and the arc length along the curve. This aspect of Bezier- and NURBS-based machining has received the most discussion in the literature.

The correct parameter must be selected based on a desired arc length along the curve. The parameter is then used to evaluate the curve yielding the waypoint.

Most papers use extrapolative techniques to predict the necessary parameter. Horsch and Jüttler [13] used a tangent-based method with parameter correction supplied by the Regula Falsi method. Yang and Kong [37] use either tangent-magnitude or second-order derivatives to do the prediction. Taylor expansions were used by Zhang and Greenway [42], Shpitalni et al. [30], Yeh and Hsu [39], Tsai and Cheng [32] to do the prediction. Yeh and Hsu [39] used a second Taylor expansion to correct for the parameter error. Tsai and Cheng [32] developed an analysis of the convergence rate of their algorithm.

Interpolation-based approaches are also used. Günter and Parent [12] devised a lookup table method that calculates arc length by Gaussian Quadrature. They divide the curve into several intervals based on the accuracy of the quadrature method and, given an arc length, perform Newton-Raphson iteration on the subinterval to find the corresponding parameter. Yang and Red [38] combined the algorithm of Günter and Parent [12] with a predictor-corrector based on an extrapolative Lagrange curve predictor and a Taylor series-based corrector. Bemporad et al. [2] use an algorithm to get an upper bound on the parameter and then do a binary search until the available calculation time is exhausted

Other methods (Wang and Yang [35], Farouki and Shah [11]) use their own curve definitions to make the correlation between arc length and parameter easier. These algorithms are not transferable to general Beziers.

2.2 SPEED PROFILES

Regulation and planning of the tool speed is done through speed profiles, which are mathematical descriptions of speed as a function of time. The two most common speed profiles are the trapezoidal profile, which is a piecewise linear curve that yields velocity continuity, and the s-curve profile, which is a piecewise quadratic curve that yields velocity and acceleration continuity. Fig. 2.1 gives simple examples of these two profiles. Fig. 2.1a shows the trapezoidal profile, Fig. 2.1b shows the accompanying acceleration profile. Figs. 2.1c through 2.1e show the s-curve profile with the accompanying acceleration and jerk profiles (jerk is the time derivative of acceleration).

As an example of how speed profiles are used, a line of length S_L is to be traversed, starting and ending at rest, using a desired speed V_d and desired acceleration A_d with a trapezoidal speed profile. In order to traverse the line in a controlled fashion, a speed profile must be constructed such that the area under the speed profile is equal to S_L. This is illustrated in Fig. 2.2. The speed profiler attempts to reach V_d using the acceleration rate A_d. If it is possible to accelerate to V_d and decelerate to zero in the length available (i.e. the length S_P required to traverse the speed profile is less than S_L), as in Fig. 2.2a, the speed profiler then adds a constant speed portion sufficient to cover the remaining length (Fig. 2.2b). If it is not possible to reach V_d within S_L, the speed profiler achieves the highest speed possible within S_L (Fig. 2.2c).

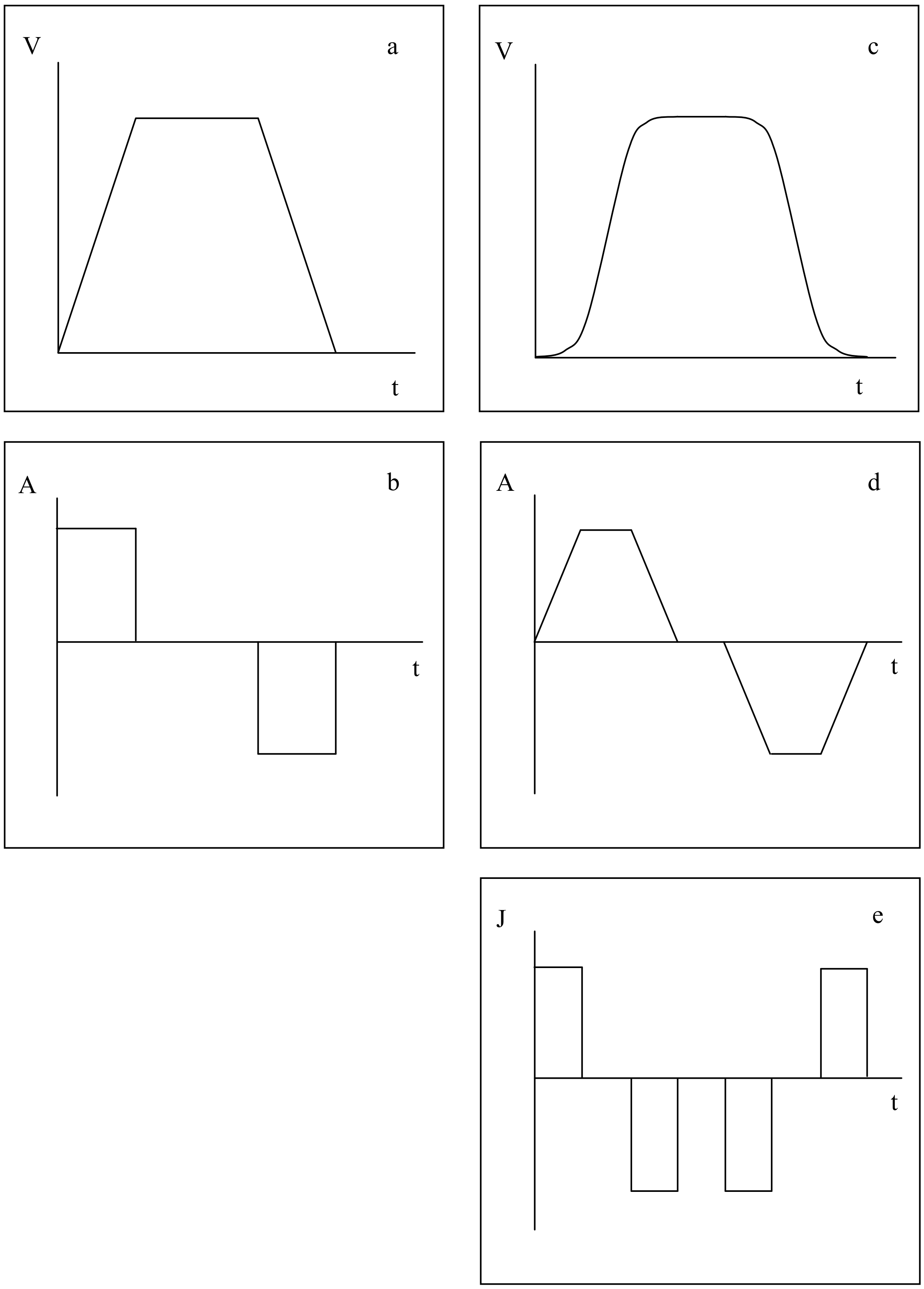

Figure 2.1. Trapezoidal and s-curve speed profiles.

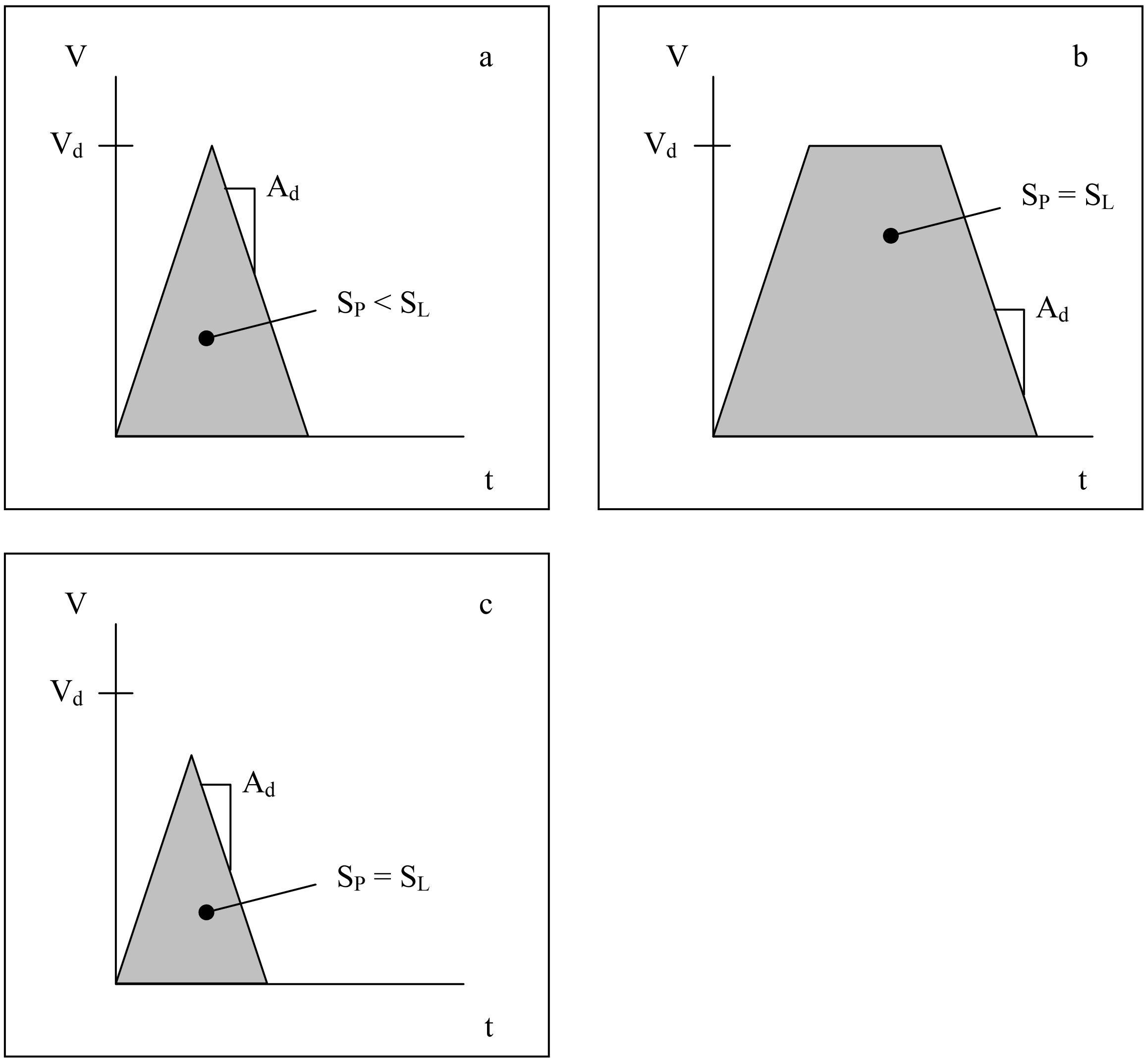

Figure 2.2. Construction of a simple speed profile.

The same basic process outlined above must be done for all the moves in a process plan. The difference being that the speed does not begin and end at zero for each move segment. Additionally, each move can have a different desired speed and length and the speed that the machine can traverse each segment can vary. A machine controller must successfully generate speed profiles on-line while maintaining smooth, continuous motion. Most of the literature on this subject is relatively basic, showing how to set up simple profiles but not discussing the intricate logic needed to robustly define useable profiles over multiple moves of varying length and dynamic requirements, such as those found in machining process plans.

Using jerk limited profiles, Red [24], Erkorkmaz and Altintas [8], and Nam and Yang [22] show how to compute the distance it takes to achieve a speed given a starting speed and simultaneously calculate the profile. Each of these papers takes a different approach but they all end up doing about the same thing, with Red [24] taking it one step further to allow for nonzero starting acceleration.

Recent research has been focused on generating optimal or near-optimal speed profiles for single moves, meaning that the process plan is executed as quickly as possible, subject to process constraints and the dynamic limitations of a given machine. Renton and Elbestawi [24] developed a two-pass algorithm that determines a minimum time speed profile subject to speed and acceleration constraints. The method is computationally expensive and determines the speed profile in the parametric domain. Dong and Stori [7] extended Renton and Elbestawi's method to account for and limit the effects of actuator limitations on contour error during path following. Timar et al. [31] developed a method for time-optimal speed profiles for single moves subject to speed and acceleration constraints. The method develops piecewise rational functions which are the square of the time-optimal feed rate.

2.3 LIMITING DYNAMICS

Closely related to speed profiling is the limiting of machine dynamics. Speed, acceleration, and jerk must be modulated appropriately to keep the forces on the machine, tool, and workpiece within required parameters and to control vibration. This is a difficult topic, and most papers on NURBS control avoid it completely.

Liu et al. [21] used a look-ahead buffer of set points and a Fast Fourier Transform to detect high jerks. They then smooth out the movement to correct for the excessive dynamics. This method is not completely geometry-based since it requires pre-tessellation. It only applies to instantaneous jerks such as corners and does not apply to jerk encountered in smooth portions of a path. Chou and Yang [6] derive the kinematics of motion for a NURBS tool path and relate them to the dynamics of a 3-axis machine tool. Yang and Chou [36] show how to analyze the resultant dynamics imposed on a machine tool when applying a given speed profile to a path.

3 METHOD: PARAMETER SELECTION

This chapter presents a method for choosing a parameter value that is associated with a specified length along a curve. Choosing a correct parameter value is necessary to ensure the desired speed is being followed, to maintain smooth motion, and to avoid unnecessary forces and vibrations. Two questions are immediately apparent. Should speed be controlled according to arc length or according to the actual point-to-point distance traveled by the tool, and what performance requirements are necessary for the method?

As shown in Fig. 1.3, the motion planner outputs set points to the servo control. The purpose of the servo control module is to track these set points while automatically compensating for unmodeled system dynamics and external inputs such as resistance to the tool, mechanism friction, and workpiece inertia.

Modern servo control is done in a point-to-point, or tessellated, fashion. The servo controller attempts to follow the set points in straight-line motions. This differs from the ideal curvilinear motion. It is therefore logical to inquire if the speed should be controlled based on curvilinear distance between set points or on the straight-line distance between set points. The straight-line distance will yield a more accurate speed, while the curvilinear distance will yield a slightly lower-than-expected actual speed, due to the fact that the curvilinear distance is equal to or higher than the straight-line distance. From this point of view it is appealing to use the straight-line distance, but another problem is more critical.

Speed profiles (see Chapter 4) govern the rate at which each move segment is traversed. These are computed using the curvilinear distance of the move segment. If straight-line distance is used to control speed, the end of the move will be reached before the speed profile is complete. This causes speed discontinuities at the junctions between move segments. Using curvilinear distance will allow for continuous speed transitions and will maintain smooth motion. Therefore the curvilinear distance is used to control speed.

The selection of a method for choosing parameter values must take into account the real-time nature of machine control. The servo control operates on a timer, accepting set point data from the motion planner at a specified frequency. The set points must arrive on time since the servo control is always trying to move to the most recent set point. If the next set point does not arrive, the servo control will attempt to maintain the most recent commanded position, essentially bringing motion to a halt in a single time step. When the next set point finally arrives, the servo control will attempt to continue motion at the previous speed, causing high accelerations. These rapid changes stress the mechanism, causing premature wear, disrupt the manufacturing process, and can cause catastrophic damage in the worst case. The algorithms used to select the parameter must therefore be bounded so a timer frequency can be selected. Higher frequencies will yield a denser tessellation of the curve, giving better resolution to the servo control and resulting in smoother motion and better tracking of the curve. It is therefore desirable to have a fast algorithm with a known maximum computation time.

Section 3.1 explains the difficulties associated with choosing the correct parameter. The nonlinearities involved in the calculations are presented with a brief discussion of the requirements for an effective algorithm. Section 3.2 presents the method for choosing the correct parameter.

3.1 THE NONLINEAR PROBLEM

With parametric curves such as Bezier and NURBS curves, the relationship between the parameter and the length along the curve is nonlinear (see Farouki [10]). Fig. 3.1 illustrates this, showing the variation of the parametric-Cartesian speed relation (ratio of change in length to change in parameter) for the Bezier curve shown in Fig. 3.2, whose control points are listed in Table 3.1. Specifically, the speed at which a curve is traversed is related to the speed at which the parameter domain is traversed by

$$V = S'(u)\dot{u} \tag{3.1}$$

where

$$S'(u) = \left\| \mathbf{P}'(u) \right\| \tag{3.2}$$

Table 3.1. Cartesian coordinates of control points for example Bezier curve.

Control Point #	X	Y	Z
1	1	2	2
2	2	5	78
3	4	6	3
4	5	3	4

So if the Bezier curve in Fig. 3.2 is defined in millimeters and the curve is traversed at a constant parametric rate of $\dot{u} = 1/S$, then the Cartesian speed varies between a maximum of 230 mm/s and a minimum of 6 mm/s.

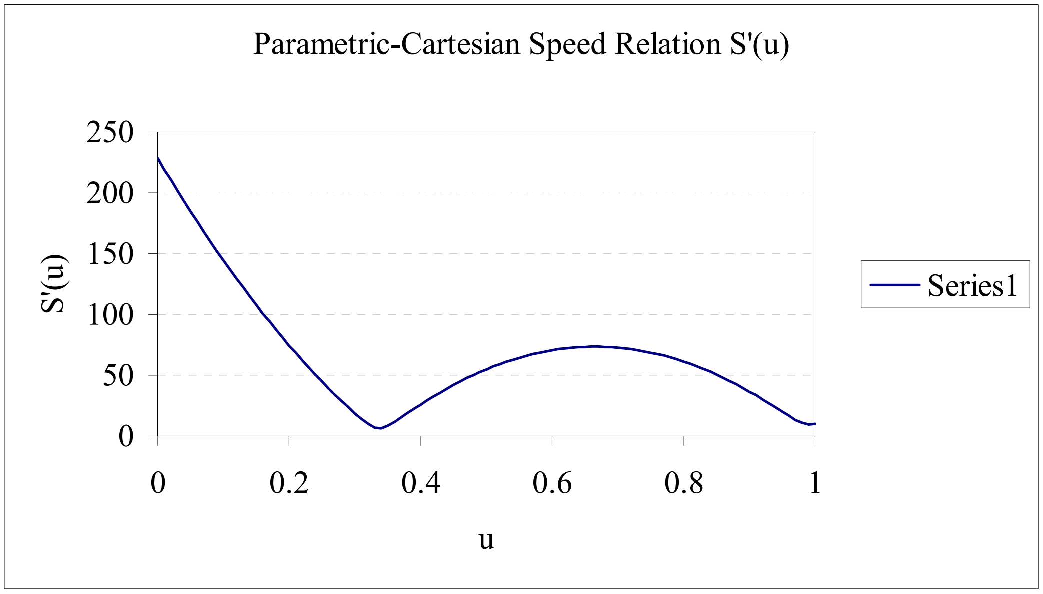

Figure 3.1. Nonlinear relationship between parameter u and parametric-Cartesian speed ratio.

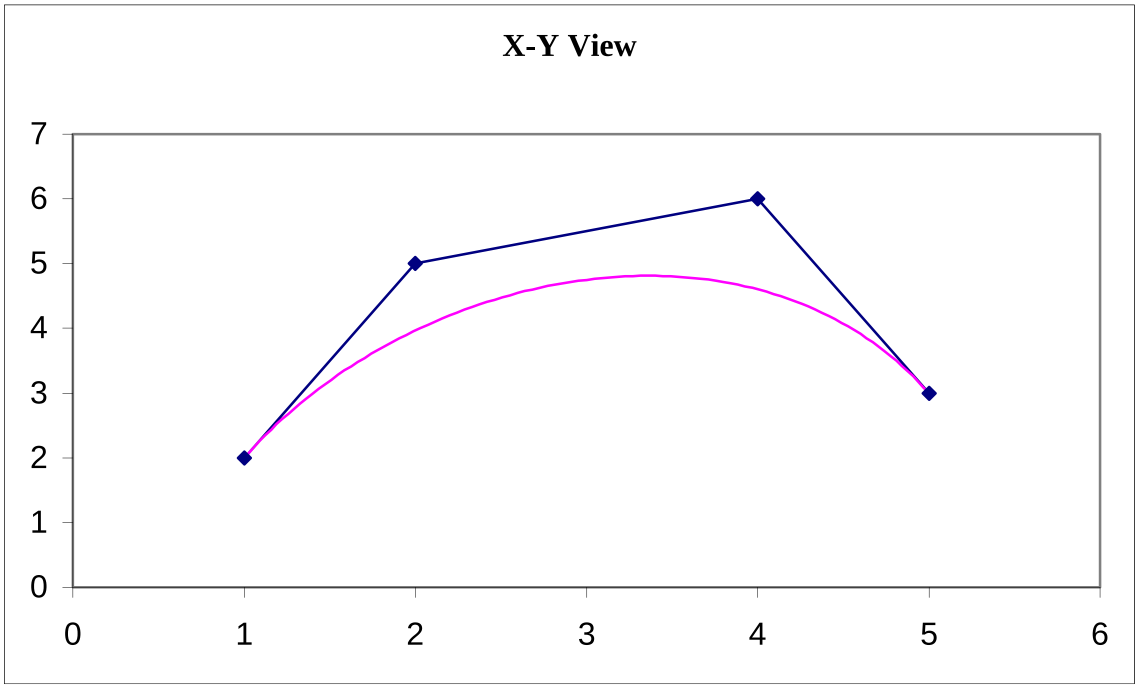

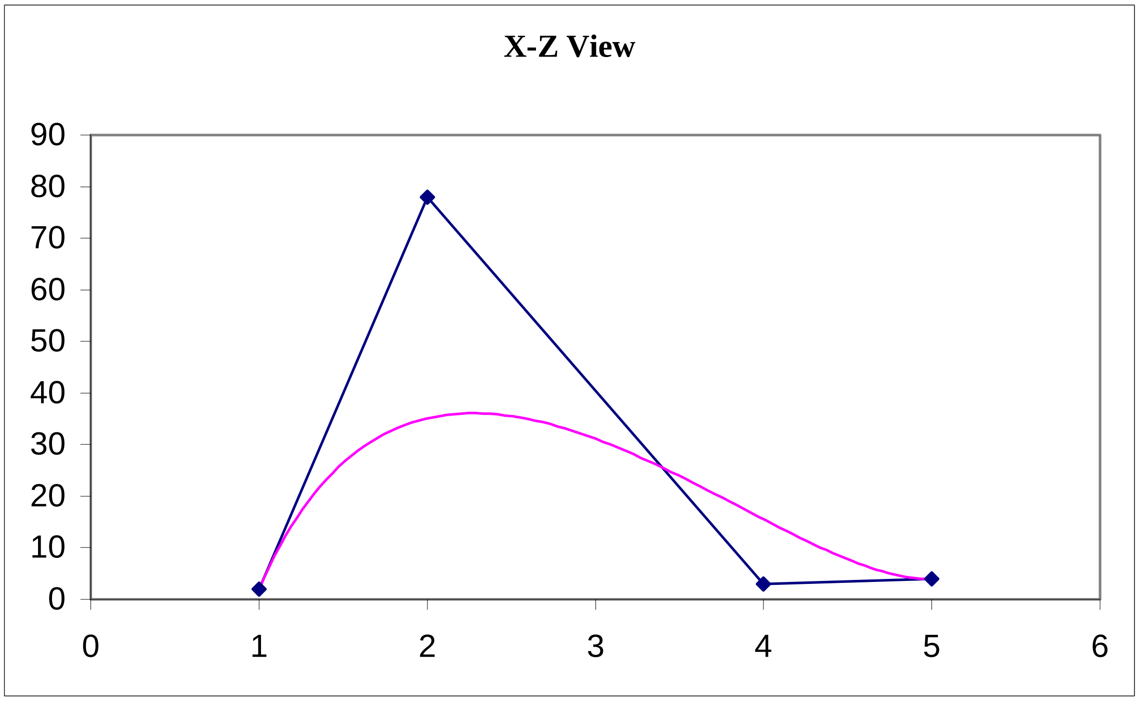

Figure 3.2. Example Bezier curve with control polygon.

In digital motion control, points along a path are specified at discrete time intervals. To specify a point $\mathbf{P}_i$ on a parametric curve $\mathbf{P}(u)$ such as a NURBS or Bezier, an appropriate parameter value u_i must be chosen that matches the desired length along the curve S_i. To do this, the relationship (3.3) between the parameter value u and the length S(u) along the curve must be resolved.

$$S(u) = \int_{u_0}^{u} S'(u)du \tag{3.3}$$

Since (3.3) cannot be solved in closed form, u_i cannot be calculated exactly without resorting to iterative methods. Due to the real-time nature of machine control, calculation time must be made deterministic by avoiding iterative methods, but errors in u_i will negatively affect motion dynamics and must be controlled. These effects can be kept within acceptable levels if the controller can specify the maximum length error ε_{length}, where

$$\varepsilon_{length} \geq \left|S(u_i) - S_i\right| \tag{3.4}$$

To do this, some iteration will be necessary, so to satisfy the requirements of real-time control, a method with rapid convergence must be used.

Previous efforts to tackle this problem [2, 11-13, 30, 32, 35, 37-39, 42] yielded algorithms that are either nonlinearly extrapolative (and thus inherently unstable) or highly iterative (such as first-derivative extrapolations and interval halving methods).

While the latter may seem attractive at first due to the simplicity and speed of such algorithms, their overall calculation time can quickly surpass that of more complicated methods since (3.3) must be evaluated as part of every iteration and checked against (3.4).

3.2 METHOD

To develop a stable, fast algorithm that minimizes iteration, this thesis uses modified versions of [12] and [38]. A basic predictor-corrector algorithm, such as is found in [38] is outlined in Fig. 3.3. First, the curve is initialized and a lookup table for the parameter-length relationship is populated. When a length command comes down, a prediction is made for the corresponding parameter. A length check is performed to confirm the accuracy of the parameter. If the parameter does not hold the required tolerance, a correction operation is performed. The check and correction are repeated until the tolerance or some other criterion is met, such as a limit on the number of iterations. Then the parameter is passed on and is used to establish the next waypoint.

The same basic approach Fig. 3.3 will be used in this method to calculate the parameter. The remainder of this chapter develops improved prediction and correction steps. Section 3.2.1 reviews the Length Calculation method of Günter and Parent [12]. Section 3.2.2 outlines a method of establishing a lookup table for the parameter-length relationship, which will be used in the prediction and correction steps. Section 3.2.3 presents an interpolative prediction method using a monotonic curve scheme. Section 3.2.4 gives a simple method for reducing the parameter error to an acceptable level.

3.2.1 LENGTH CALCULATION

The first thing a predictor-corrector needs is a reliable way to calculate the length along a curve (the arc length) at a parameter value. This is done by integrating (3.3). Günter and Parent [12] developed such a method using a lookup table and Gauss-Legendre quadrature, and the method was clarified by Yang and Red [38], which also added an error analysis. This method is reviewed here, with minor changes.

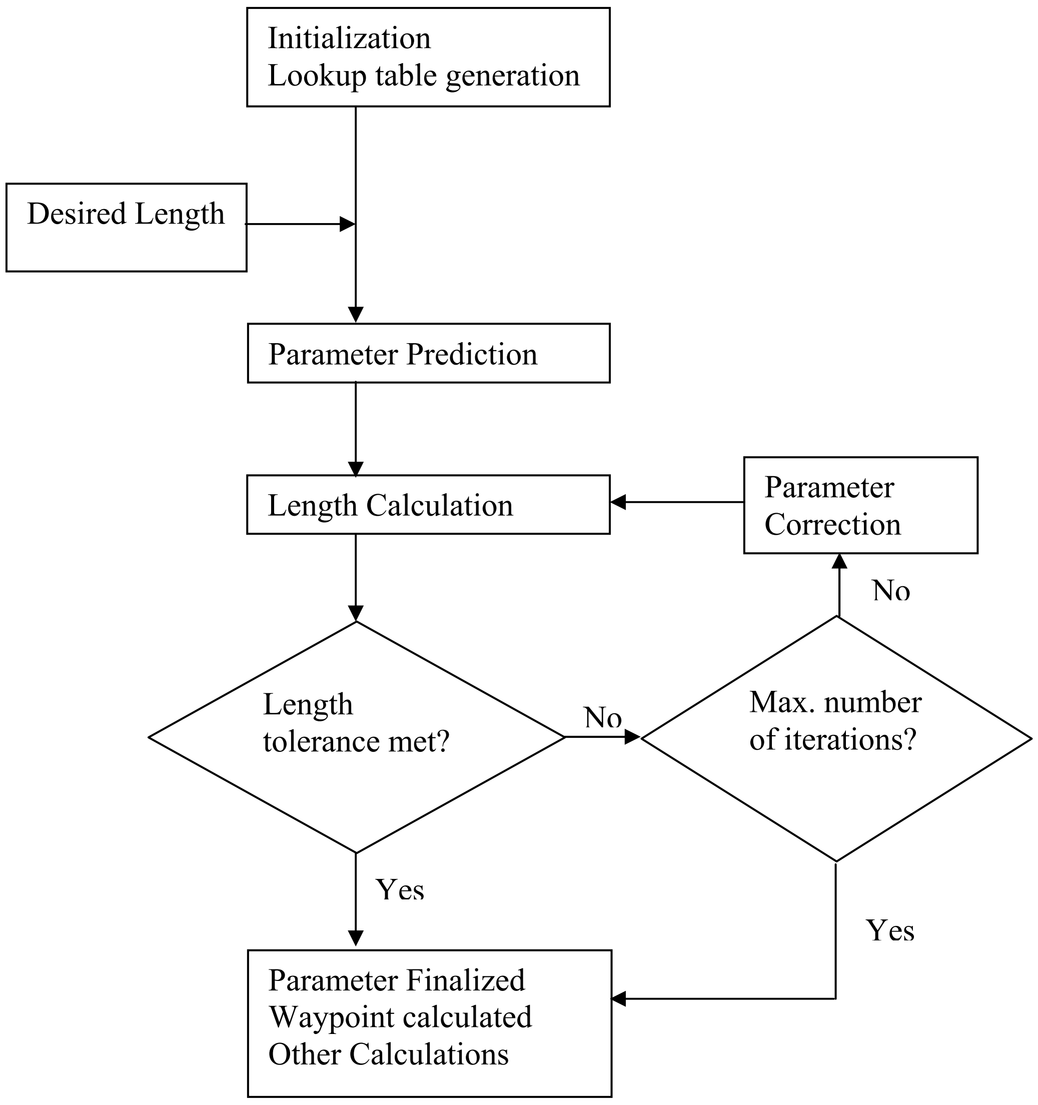

Figure 3.3. Typical predictor-corrector algorithm.

Gauss-Legendre quadrature is a numerical method of integration that is exact for polynomials of degree ≤ (2n-1), where n is the degree of the quadrature. Gauss-Legendre quadrature integrates a function by summing weighted evaluations of that function. If the function S′(u) is to be integrated over an arbitrary interval u=[a,b], the quadrature equation is

$$\int_a^b S'(u)\,du = \sum_{i=0}^{n} w_i S'(u_i) + \varepsilon(S', n, a, b) \tag{3.5}$$

where ε(S′,n,a,b) is the error function and w_i are tabulated weights. From Kythe and Schaeferkotter [19]:

$$u_i = \frac{(b-a)x_i + (b+a)}{2} \tag{3.6}$$

$$\varepsilon(S', n, a, b) = (b-a)^{2n+1} K_n\, S^{(2n+1)}(\xi) \tag{3.7}$$

where $\xi \in (a,b)$,

$$K_n = \frac{2^{2n+1}(n!)^4}{(2n+1)[(2n)!]^3} \tag{3.8}$$

and x_i and w_i are tabulated constants that depend on the degree of the quadrature. These constants can be found in most texts that deal with Gaussian quadrature, such as [19].

3.2.2 LOOKUP TABLE

The first thing that must be done in establishing a lookup table is to determine the number of entries that are needed. The error function (3.7) can be used to do this.

The value $S'_{max} = \max[S^{(2n+1)}(\xi)]$ can be substituted into (3.7) to find the number of divisions in the lookup table necessary to hold the length-calculation error:

$$N_{table} = \frac{(b-a)^{2n+1} K_n S'_{max}}{\varepsilon_{length}} \tag{3.9}$$

Using N_{table} (rounded up to the next largest integer) to calculate the parameter interval Δu on which to set up the lookup table:

$$\Delta u = \frac{b-a}{N_{table}} \tag{3.10}$$

A quadrature operation is performed on each interval to populate the "Length" column of the lookup table, as in Table 3.2.

Subsequent length calculations are performed on a subinterval. For example, if a parameter u is chosen such that $u_i < u < u_{i+1}$, then the quadrature operation will be performed on the interval $[u_i, u]$ and the result added to S_i.

Table 3.2. Lookup table for parameter-length relationship.

Node	**Parameter**	**Length**
0	a	0
1	u_1	S_1
...	...	...
$N_{table}-1$	$u_{Ntable-1}$	$S_{Ntable-1}$
N_{table}	b	$S_{Ntable} = S(b)$

3.2.3 PARAMETER PREDICTION

With a lookup table established, a method must be defined to predict a parameter u given a desired length S. Some predictors use a first- or second-order Taylor expansion or a tangent magnitude method of prediction. Other papers use polynomial predictors based upon previous waypoints. Yang and Red [38] used Lagrange interpolation over previous waypoints to predict the next waypoint parameter. Second-order expansions and polynomial predictors have the disadvantage of doubling back, i.e. they can reach a point where an increase in length results in a decrease in parameter, as in Fig. 1.4. This is not representative of the monotonic nature of (3.3) and can easily defeat the prediction scheme. First-order and tangent magnitude methods may suffer from low convergence rates. All current methods in the literature are extrapolative.

The current methods in the literature usually work for step sizes that are small in relation to the length of the curve. However, as the step sizes increase, the extrapolations break down. A prediction method will now be presented that is both interpolative and representative of the monotonic nature of (3.3). This method is stable and will provide better convergence rates for larger step sizes.

Sarfraz [27] developed a curve definition with specifiable endpoints and derivatives. This curve is guaranteed to be monotonic. An interpolative prediction method using a monotonic curve with specifiable end conditions will generally follow the length curve better than extrapolative polynomial and derivative methods, as illustrated in Fig. 3.4.

The Sarfraz curve is a rational cubic spline that is guaranteed to be monotonic. While the curve is presented in [27] as a spline, for clarity it will be defined here as an individual curve segment (3.12). Some minor simplifications are also made that result from the constraints of the present application. Given endpoints (S_0, u_0), (S_1, u_1) and derivatives d_0 and d_1 where

$$d_i = \frac{1}{S'(u_i)} \tag{3.11}$$

the Sarfraz curve is defined as

$$u(S) = u_0(1-\theta) + u_1\theta + \frac{\theta(1-\theta)^2([S_1 - S_0]d_0 - u_1 + u_0) + \theta^2(1-\theta)(u_1 - u_0 - [S_1 - S_0]d_1)}{(1-\theta)^3 + \omega\theta(1-\theta)^2 + \omega\theta^2(1-\theta) + \theta^3} \tag{3.12}$$

$$\theta = \frac{S - S_0}{S_1 - S_0} \tag{3.13}$$

$$\omega = \frac{(d_1 + d_0)(S_1 - S_0)}{u_1 - u_0} \tag{3.14}$$

The monotonicity of this curve is proven in [27].

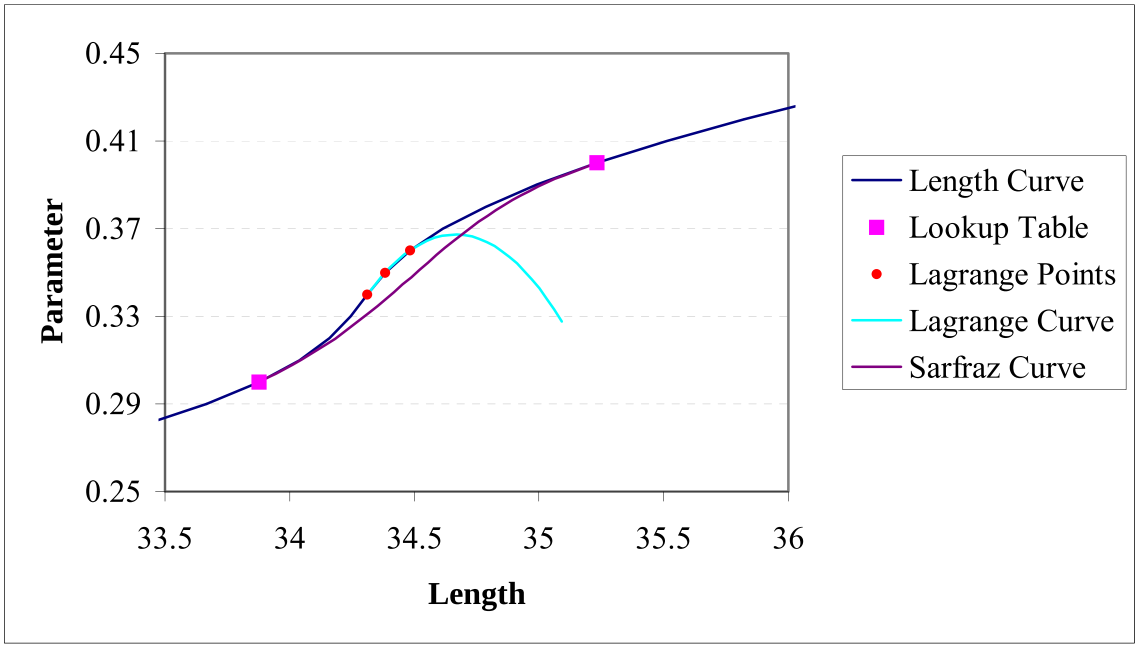

Figure 3.4. Comparison of Lagrange curve and monotonic Sarfraz curve for parameter prediction.

To predict a parameter value, the lookup table is searched to find the interval on which the desired length resides. Using the endpoints of this interval and the corresponding derivatives, a Sarfraz curve segment is set up over the interval. Evaluating the Sarfraz curve at the desired length yields a parameter prediction. The actual length along the curve at the predicted parameter can be obtained by performing a quadrature operation from the beginning of the interval to the predicted parameter.

3.2.4 PARAMETER CORRECTION

The predicted parameter may violate the length tolerance ε_{length}. In this case a correction operation must be performed on the predicted parameter. This is easily done by setting up another Sarfraz curve. If the predicted parameter is too high, the new Sarfraz curve is set up between the beginning of the table interval and the predicted parameter. If the predicted parameter is too low, the new Sarfraz curve is set up between the predicted parameter and the end of the table interval. The new parameter is then predicted. If necessary, another Sarfraz curve can be set up for another prediction. If this method is combined with simple interval halving, the convergence rate is very rapid. The method is also algorithmically stable.

4 METHOD: SPEED PROFILING

This chapter presents a method for planning the speed along a curve. Planning speed is important for generating smooth accelerations and decelerations and for respecting dynamic limitations on the machine and the manufacturing process.

Section 4.1 presents the definition of a simple jerk-limited speed profile. Section 4.2 explains the dynamic limitations a set of moves places on the speed profile. Section 4.3 defines a speed profiling algorithm that meets the requirements of real-time control.

4.1 THE JERK-LIMITED SPEED PROFILE

In machining operations, a desired tool tip speed is specified for any particular portion of the process plan. However, each machine has its own dynamic limitations, so the tool cannot always be moved at the desired speed along the entire path. Thus, the controller's job is to control the tool as close to the desired speed as possible while respecting machine limitations. This is accomplished by the proper construction and following of speed profiles. A speed profile is a map of the speed across an individual move or set of moves.

Trapezoidal profiles used to be the norm in machine control. Over time the jerk capabilities of motors advanced to the point where they began to stress mechanisms, causing premature wear. Jerk is the time derivative of acceleration and can be thought of as a measure of impact. Jerk-limited speed profiles were developed to reduce these stresses. A typical jerk-limited speed profile section and its derivatives are defined by the following time-dependent equations

$$S(t) = S_{start} + V_{start}t + \frac{A_{start}t^2}{2} + \frac{J_0 t^3}{6} \tag{4.1}$$

$$V(t) = V_{start} + A_{start}t + \frac{J_0 t^2}{2} \tag{4.2}$$

$$A(t) = A_{start} + J_0 t \tag{4.3}$$

$$J(t) = J_0 \tag{4.4}$$

Note that if $J_0 = J_{max}$, the speed profile allows for the optimal (shortest) transition time between speeds. Therefore, the maximum allowable jerk is always used.

Jerk-limited speed profiles consist of seven types of profile sections, classified by their shape and behavior. These types are listed below and represented in Fig. 4.1.

1) Concave Rise
2) Linear Rise
3) Convex Rise

4) Constant Speed

5) Convex Fall

6) Linear Fall

7) Concave Fall

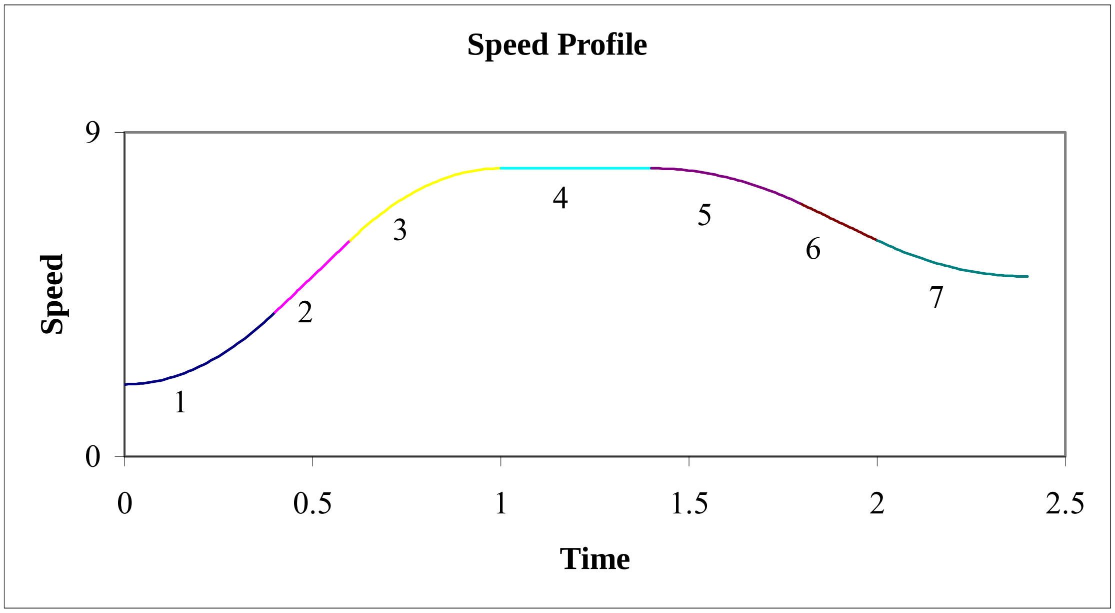

Figure 4.1. The seven types of speed profile sections.

Setting up speed profiles of this nature is relatively straightforward using algorithms currently found in the literature (Red [24], Erkorkmaz and Altintas [8], Nam and Yang [22]). A more difficult problem is maintaining the desired speed while handling sequential moves of all sizes and dynamic requirements. Indeed, defining the logic necessary to create a robust speed profiler is a much more rigorous task than defining the mathematics for individual profile segments. The specifics of the problem are explained in Sections 4.2 and 4.3. A solution to the problem is given in Section 4.3.

4.2 DYNAMIC LIMITATIONS ON SPEED PROFILES

Every move has its own dynamic limitations. In other words, each move interacts with the machine differently so as to limit the feasible speed, acceleration, and jerk across that move. A simple example is found in traversing a circular path at constant speed. Here, the radial acceleration A_r depends on the traversal speed V and the radius of curvature R of the path as

$$A_r = \frac{V^2}{R} \tag{4.5}$$

If there is a maximum allowable value for A_r, then it can be seen by inspection that the value of R will have an effect on the allowable values of V.

A sequence of moves may have allowable speeds resembling the contrived example in Fig. 4.2, but in the general case can take on essentially any shape. In addition to limited speed, each move will have its own limits on allowable acceleration and jerk. The calculation of these limits is discussed in Chapter 5. Since the current chapter is strictly concerned with the construction of speed profiles, it is assumed that these limits have already been calculated.

4.3 SPEED PROFILE CONSTRUCTION

Fig 4.2 shows an example of allowable (solid lines) and desired (dashed line) speeds for a set of moves. It is important to realize that the allowable speeds for one move are completely independent of every other move. Therefore the allowable speed plot can assume any configuration. A speed profiler must be able to handle any set of moves, and perform well. The problem is to construct such a speed profile over a given set of moves. The requirements are as follows:

1) Increase as quickly as possible to the desired speed
2) Maintain as close a speed as possible to the desired speed
3) Respect the allowable speeds, accels, and jerks
4) Reach zero speed by the end of the last available move

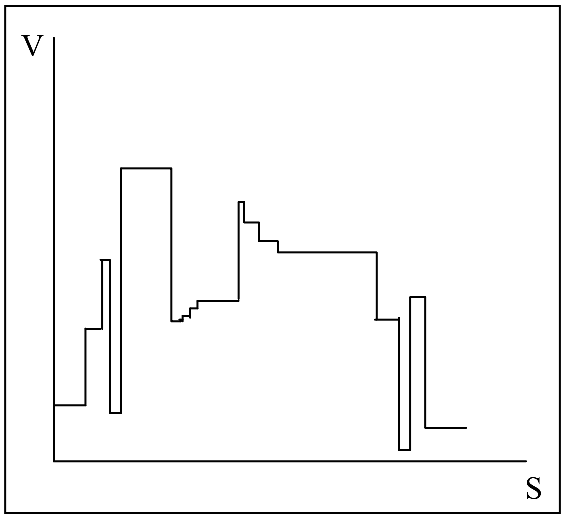

Figure 4.2. Example of allowable and desired speeds.

Requirements 3 and 4 are of particular interest. Many published algorithms use estimations of remaining length to plan their speed profiles or ignore this requirement altogether, but if the speed profile is calculated incorrectly, so that zero speed profile does not reach zero speed by the end of the move sequence, dynamic limitations will be exceeded. Additionally, most papers ignore dynamics in order to simplify the algorithms. These requirements, however, cannot be ignored in a real implementation.

In order to make the logic and accompanying explanation feasible, some simplifying constraints will be applied to the speed profiling problem. That is, zero acceleration will be specified at the endpoints of moves. This allows convergence to be guaranteed for the algorithm, without iteration. Additionally, once the waypoint enters a segment, the speed profile for that segment will not be adjusted.

The reader may assume that (referring to Fig. 4.1) accelerating profiles consist of a sequence of profile segments of types 1 and 3 and that decelerating profiles consist of profile segments of types 5 and 7. In other words, the explanations in this chapter refer to speed profiles containing "perfect S-curves", which do not contain portions of constant acceleration or constant speed. The logic for using speed profiles with constant acceleration or constant speed portions is similar to that for perfect S-curves. Including speed profiles with constant acceleration or speed would unnecessarily multiply the number of cases that need to be explained. Thus, in order to facilitate reader understanding of the underlying speed profiling concept, the specific cases for profiles including constant acceleration and speed portions are not discussed.

The algorithm comes in two parts, a forward recursion and a backward recursion, explained in detail in Sections 4.3.1 and 4.3.2. The purpose of the forward recursion is to attain and maintain the specified speed. The backward recursion ensures that allowable speeds are respected and that the speed profile can reach zero before the end of the move sequence. The backward recursion is only needed if the forward recursion fails to generate a feasible profile.

The logic for the forward and backward recursions are given in Sections 4.3.1 and 4.3.2, respectively. A pseudocode summary of the speed profiling algorithm is given in Section 4.3.3. A peculiarity of s-curve speed profiles is that the profile may have a "dead spot," a range of speed that cannot be reached with the specified acceleration and jerk. A mathematical explanation for this is given in Section 4.3.4.

4.3.1 FORWARD RECURSION

The forward recursion attempts to reach the desired speed by accelerating over one or more upcoming move segments. It then attempts to reach zero speed by decelerating over the remaining segments. This process is shown in Fig. 4.3. Each time the waypoint enters a new move segment, the speed profiler attempts to increase speed over the following move (optionally, several upcoming moves), and then decreases to zero. This also happens on the first step after starting from zero, as in Fig. 4.4. In this way, the speed profile is always increasing, but only over the minimum number of segments necessary. This allows the profile to define a path to zero speed with as little calculation time as possible. In both Figs. 4.3 and 4.4 the 'X' indicates the current position in the speed profile.

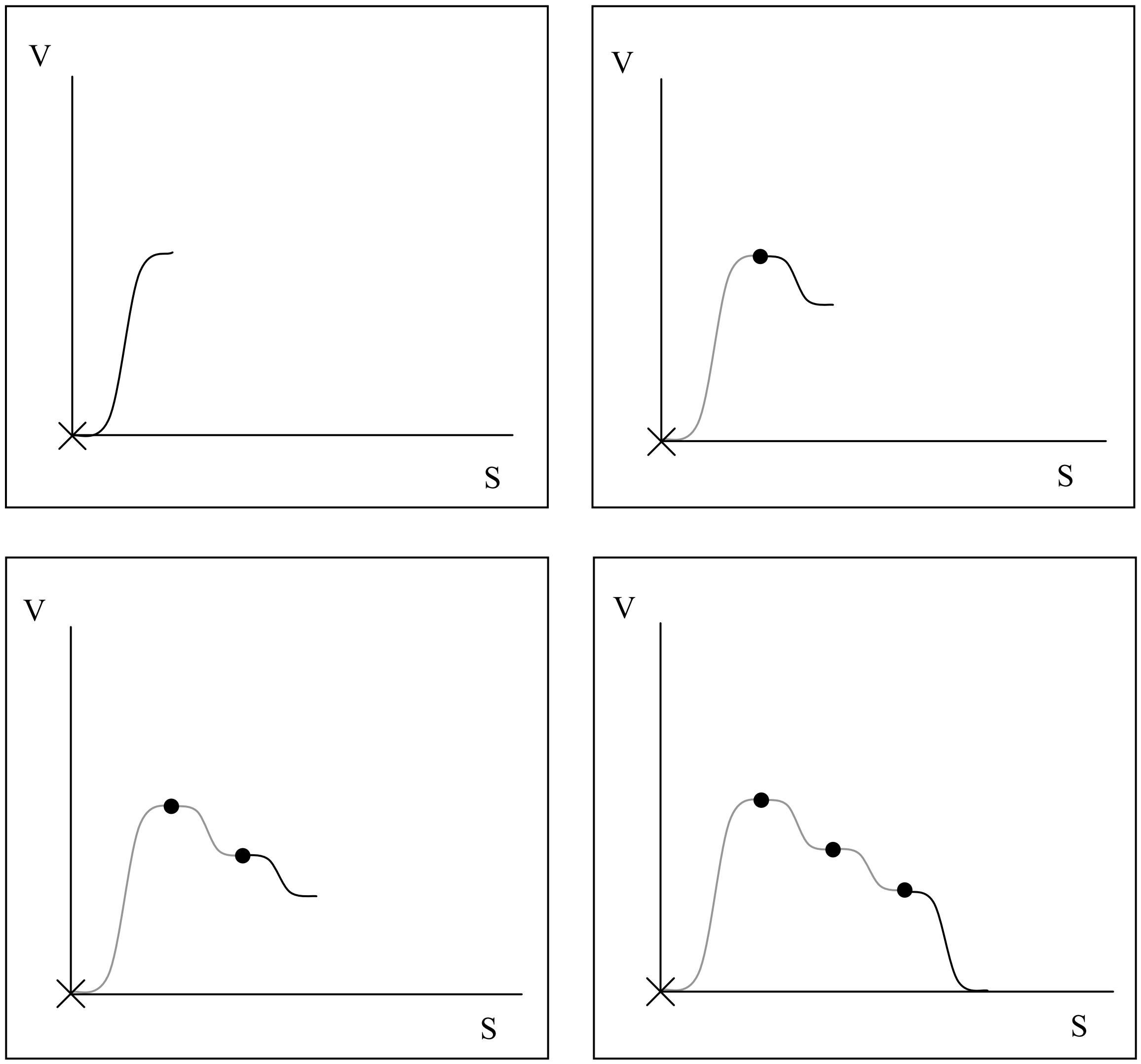

Figure 4.3. Example forward recursion beginning from zero speed.

There are a number of cases that arise during the forward recursion. These cases and the logic for handling them are presented in Section 4.3.1.1 for the acceleration stage and Section 4.3.1.2 for the deceleration stage.

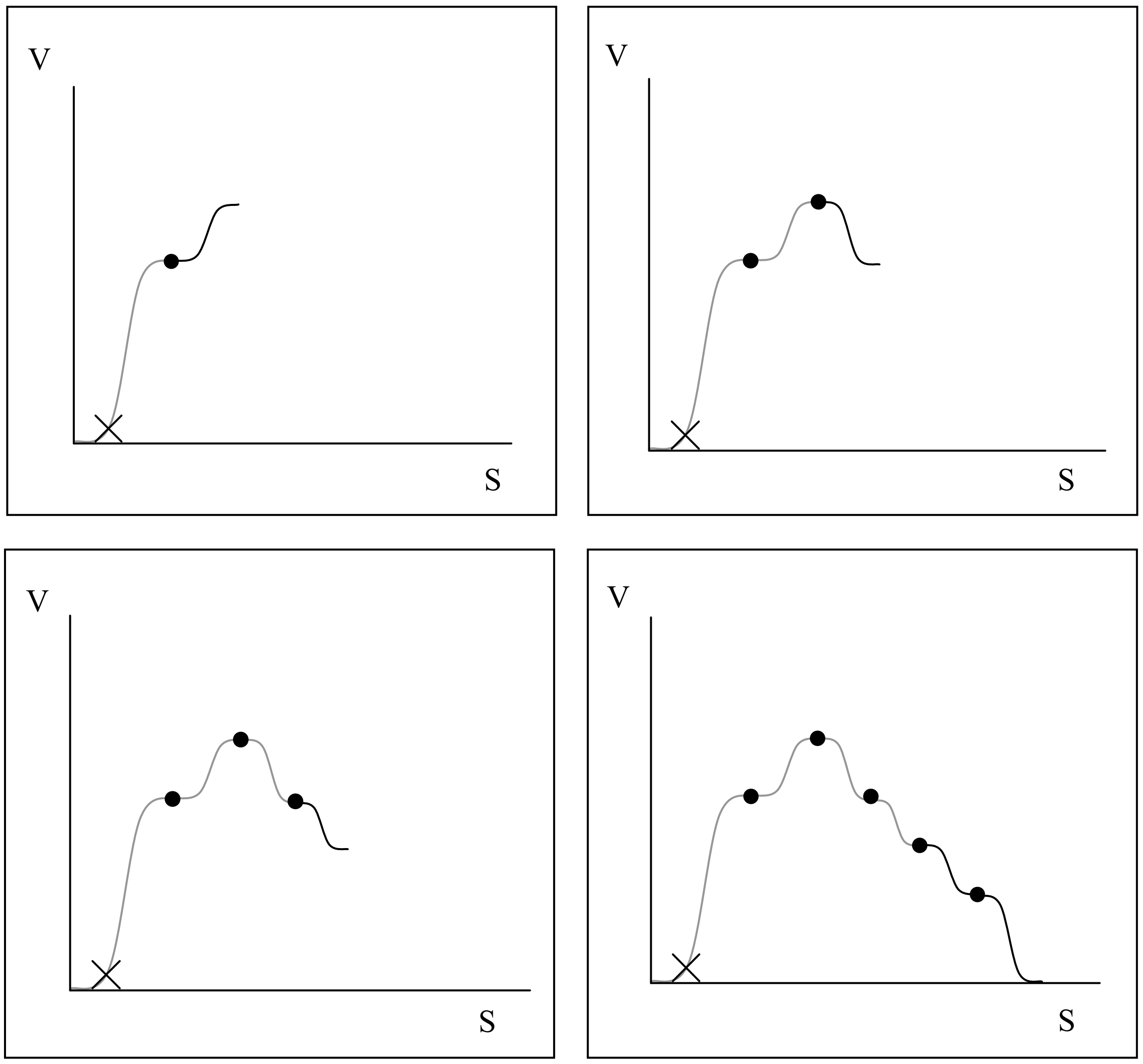

Figure 4.4. Example forward recursion upon stepping into a new move segment.

4.3.1.1 ACCELERATION STAGE

In the acceleration stage, the speed profiler attempts to reach the desired speed by increasing speed over a segment of known length. If it is necessary to decrease speed over that segment to maintain allowable speeds, the profiler tries to hold the highest acceptable speed. The cases for the acceleration stage are illustrated in Fig. 4.5, and explained below.

Cases:

a) Unobstructed – The speed profile is not constrained by allowable speeds. In this case the maximum possible speed change over the segment is used.
b) Limited – The speed change over the current move is constrained by the allowable speed, not the length of the segment.
c) Limited Decelerating – Here the allowable speed for the following segment is lower than the starting speed for the current segment. In this case, instead of increasing over the segment, the speed is reduced to the allowable speed for the following segment. This case occurs when there is sufficient length in the segment to make the change.
d) Jerk Constrained – Similar to the Limited Decelerating case in that the allowable speed for the following move is lower than the starting speed for the current move. The difference is that the quadratic nature of the speed profile comes into play. Because of the limited jerk, there are two separate regions of reachable speeds (see Section 4.3.4), so if the allowable speed for the following move is between the attainable regions, the allowable speed for the following move cannot be exactly reached. The highest possible attainable speed is chosen that is below the allowable speed for the following move.

e) Violating – The allowable speed for the following move will be violated. Here the starting speed for the following move is set to the allowable speed and a backward recursion must be performed.

f) End of Buffer – Zero speed could not be reached by the end of the last segment. The ending speed of that segment is set to zero and a backward recursion is begun.

4.3.1.2 DECELERATION STAGE

The deceleration stage is much simpler than the acceleration stage. Here the speed profiler simply tries to decrease to zero speed as fast as possible. The cases for the deceleration stage are found in Fig. 4.6, and explained below.

Cases:

a) Unobstructed – The speed profile is not constrained by allowable speeds. In this case the maximum possible speed change over the segment is used.

b) Violating – The allowable speed for the following move will be violated. Here the starting speed for the following move is set to the allowable speed and a backward recursion must be performed.

c) End of Buffer – Zero speed could not be reached by the end of the last segment. The ending speed of that segment is set to zero and a backward recursion is begun.

d) Stopped – The speed profile has reached zero speed.

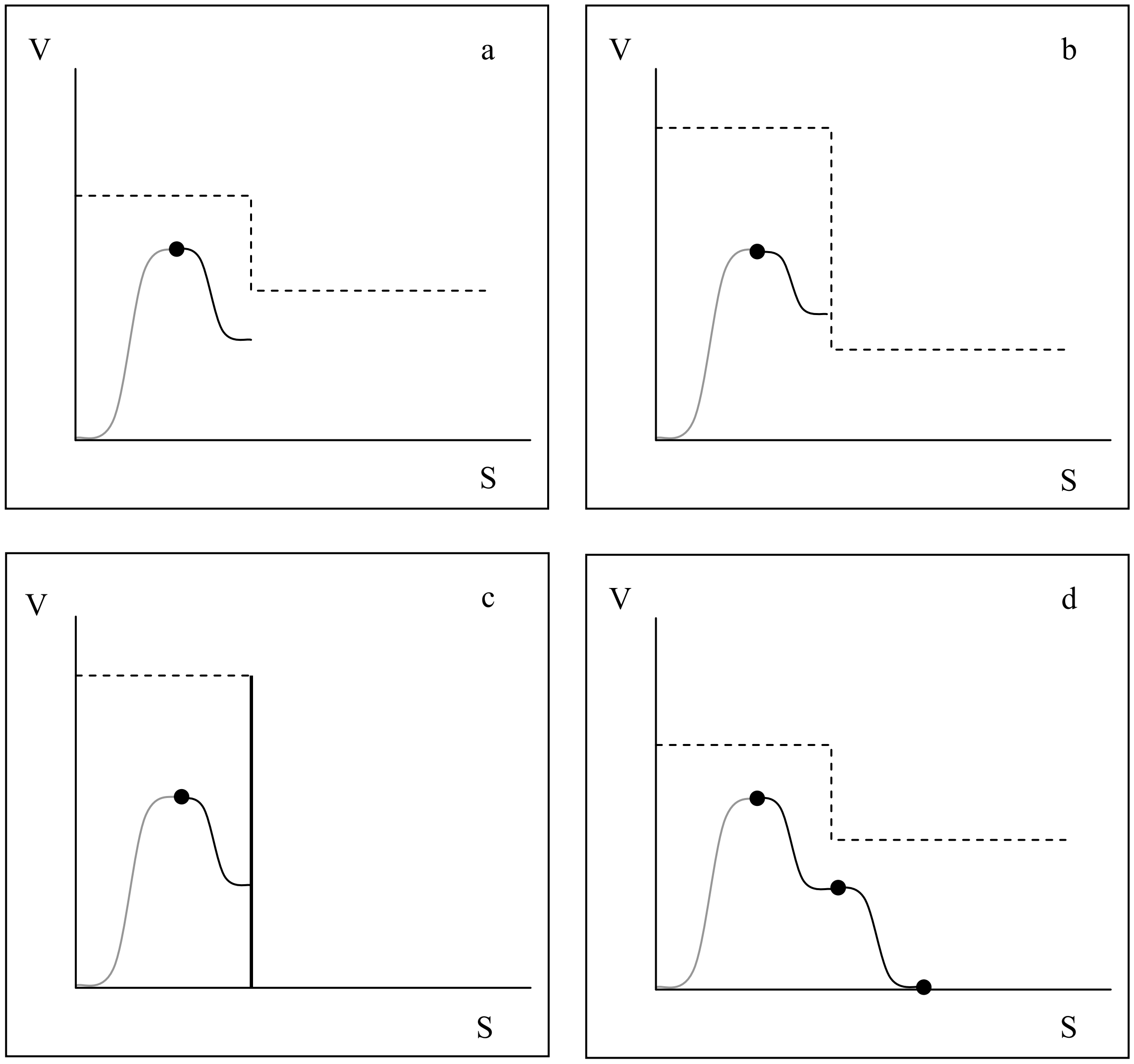

Figure 4.6. Forward recursion, deceleration stage cases.

4.3.2 BACKWARD RECURSION

The backward recursion attempts to construct a feasible speed profile when the forward recursion fails, such as when an allowable speed violation occurs (Fig. 4.7). The backward recursion begins where the forward recursion ended, at zero speed. It then constructs a speed profile in the reverse direction, always trying to "connect" with the speed profile currently in use.

There are two main cases that arise during the backward recursion, the case when the motion is starting from zero and a speed profile is not yet established, and the case when the motion is already moving on a speed profile and the motion planner is attempting to construct a new speed profile. These cases and the logic for handling them are presented in Section 4.3.2.1 for the case where a current speed profile is established and Section 4.3.2.2 for the case where there is no current speed profile in use.

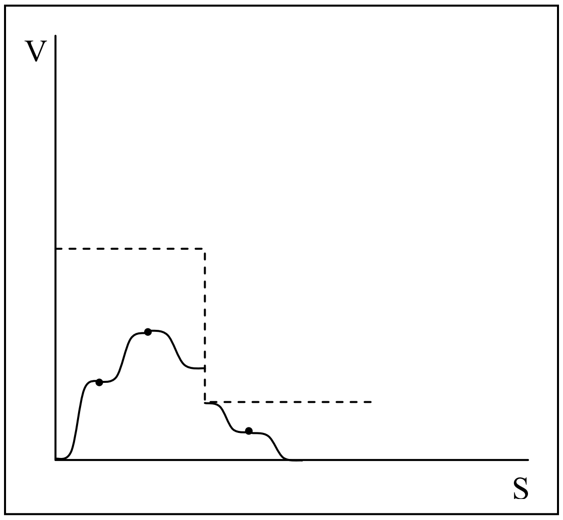

Figure 4.7. Example of a failed forward recursion.

4.3.2.1 PROFILE ESTABLISHED

If a useable speed profile has already been established, the goal of the backward recursion is to connect with that speed profile. The cases encountered are shown in Fig. 4.8, and explained below.

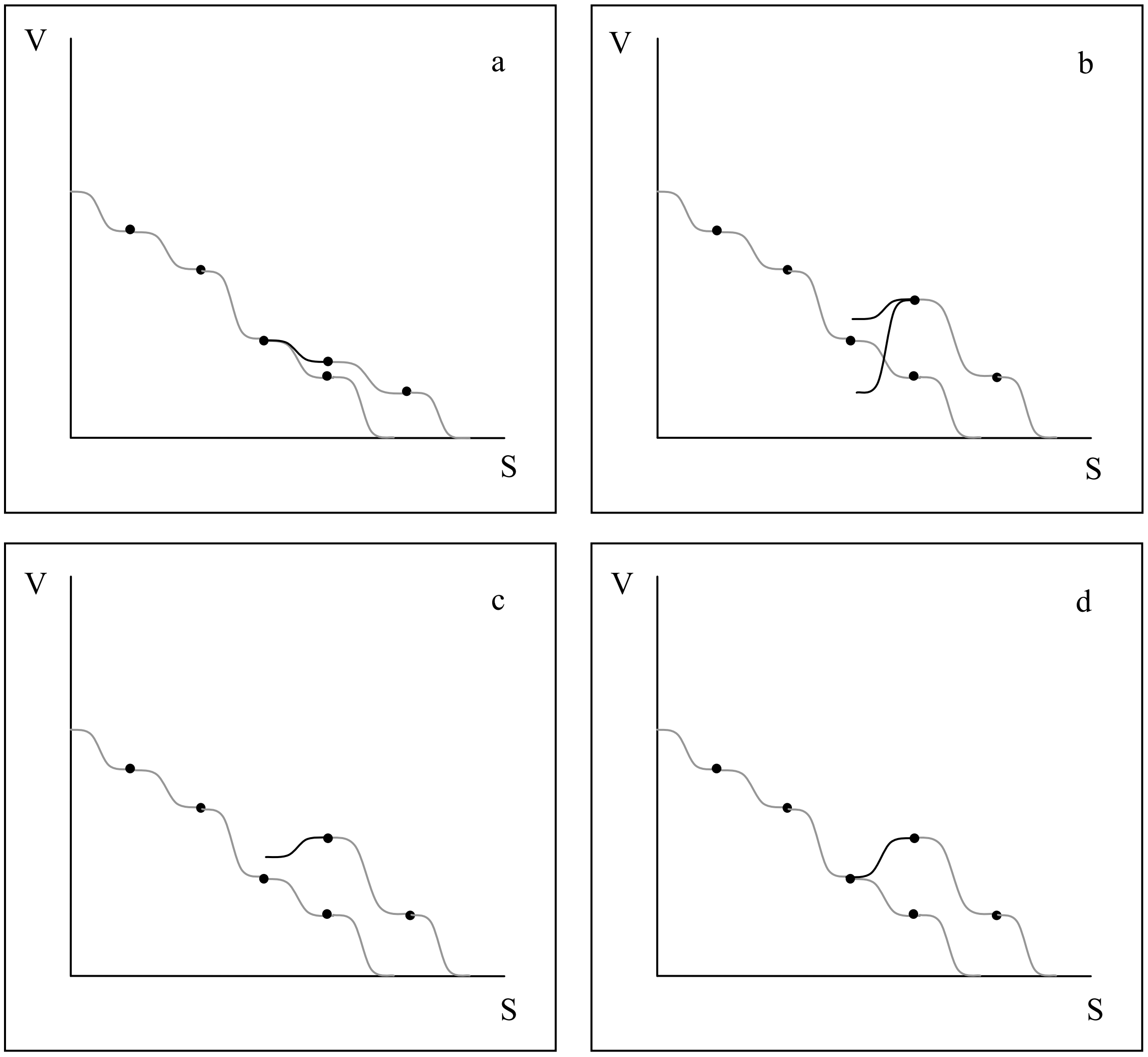

Figure 4.8. Backward recursion cases with profile established.

Cases:

a) Converged Increasing – The backward recursion converges with the established speed profile.

b) Jerk Limited – The backward recursion can reach above and below the established speed profile but cannot converge with it. Here the higher speed will be kept.

c) Decreasing – The backward recursion tries to converge with the established speed profile by decreasing speed but cannot converge. The lowest attainable speed is kept.

d) Converged Decreasing – The backward recursion converges with the established speed profile by decreasing speed.

4.3.2.2 NO PROFILE ESTABLISHED

If no useable speed profile has been established, the goal of the backward recursion is to connect with the forward recursion. Because the forward recursion can have discontinuities, if the backward recursion converges with the forward recursion, the backward recursion will still construct a full profile back to the beginning of the buffer. The cases encountered are shown in Fig. 4.9, and explained below.

Cases:

a) Nonconverged – The backward recursion does not converge with the forward recursion. In this case the highest attainable speed is kept.

b) Converged – The backward recursion can converge with the forward recursion. The backward recursion is continued, always trying to follow the forward recursion.

c) First Segment – The backward recursion reaches the first segment and decreases to zero.

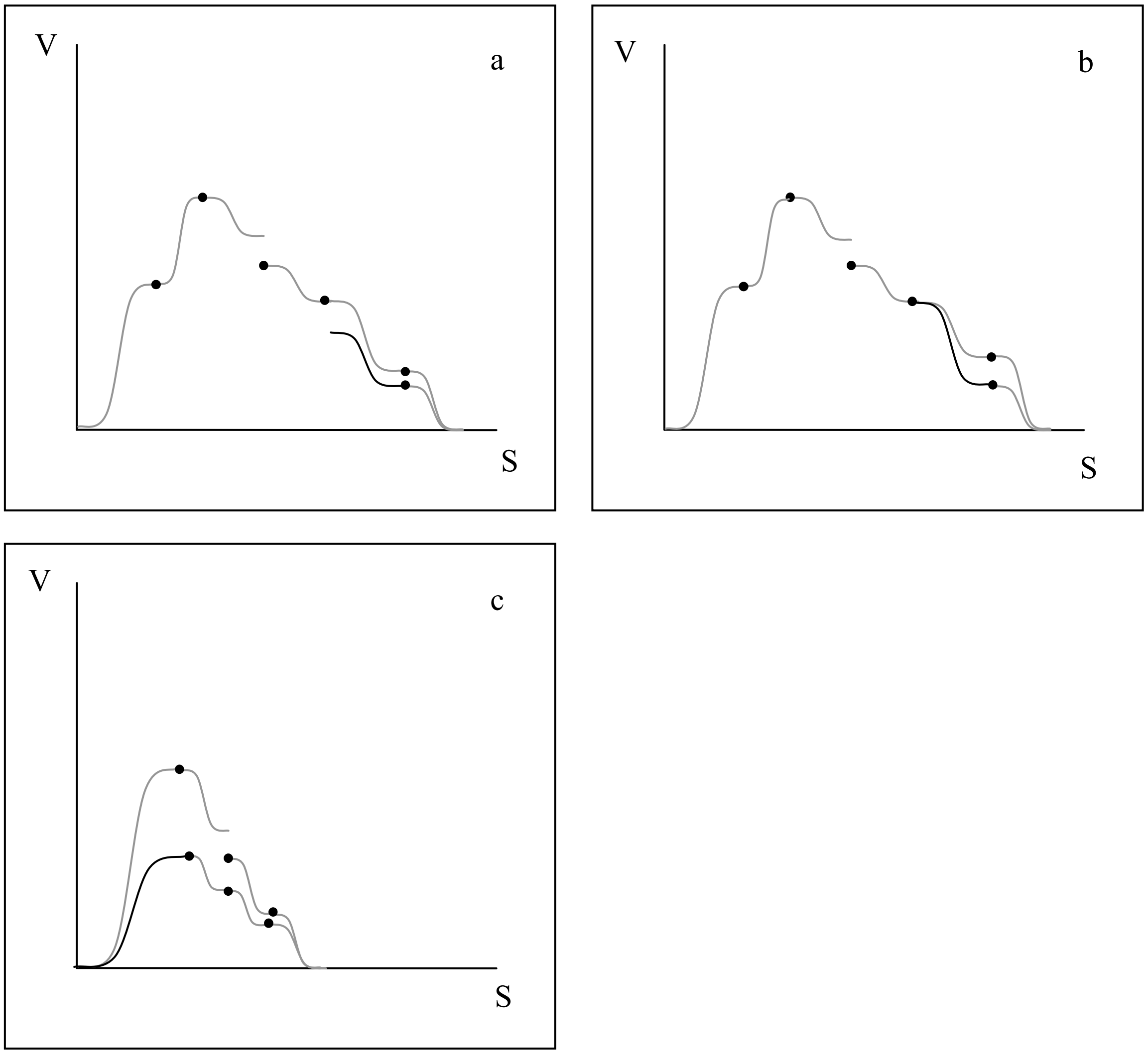

Figure 4.9. Backward recursion cases with no profile established.

4.3.3 ALGORITHM SUMMARY

Presented below is a pseudocode summary of the speed profiling algorithm.

```
//begin forward recursion
//begin acceleration phase
if Current speed is zero
  start on current segment
else
  start on segment after the current segment
Test for the highest attainable speed
if allowable speed is lower than the attainable speed
  keep the allowable speed
else
```

```
  keep the attainable speed
move to next segment
//begin deceleration phase
loop
  test for the lowest attainable speed
  if attainable speed is less than or equal to zero
    keep zero as the speed
    exit forward recursion
  else if end of buffer is reached
    keep zero as the speed
    must do a backward recursion
    exit forward recursion
  else if allowable speed is lower than the attainable speed
    keep the allowable speed
    must do a backward recursion
  else
    keep the attainable speed
    move to next segment

//begin backward recursion
if must do backward recursion
  Start at end of forward recursion
  loop
    if at current segment
      try to link with current segment starting speed
      if successful
        use backward recursion as the useable profile
        exit backward recursion
      else
        discard backward recursion
        exit backward recursion
    if No useable profile
      Test for the attainable speed
        if we can attain same or higher speed than the forward
           recursion
        if the forward recursion is lower than the current ending state
          find the low speed we can attain
          if we can reach down to the forward recursion
            keep the forward recursion value
          else
            keep the lower attainable speed
        else
          keep the forward recursion value
        else
          keep the attainable speed
    else
      Test for the attainable speed
        if we can attain same or higher speed than the useable profile
          if useable profile is higher than the current ending state
            use the rest of the useable profile
          else
            find the lowest attainable speed
            if we can reach the useable profile or lower
            if we can reach the exact value of the useable profile
              use the rest of the useable profile
            else
```

```
                keep the lowest attainable speed that is above the
                previous useable state
          else
            keep the lowest attainable speed
        else
          keep the attainable speed
    move to previous segment
else
  use forward recursion as the useable profile
```

4.3.4 JERK-CONSTRAINED DECELERATION PROFILES

A peculiarity of the jerk-limited speed profile is that, when reducing speed, there may be two disconnected regions of attainable lower speeds. It will be shown why this is, but first a few logical tools must be developed.

Recall the types of speed profile segments as presented in Fig. 3.1. The sequence of a Concave Rise speed profile section followed by a Convex Rise section (Fig. 4.10a), or a Convex Fall section followed by a Concave Fall section (Fig. 4.10b) constitutes a "perfect s-curve." These speed profile sections share a common jerk magnitude and a common maximum acceleration value. This yields the ability to simplify the equations somewhat into a set of tools.

Since the speed profile sections share a common jerk magnitude J_0 and a common maximum acceleration value A_{max}, it can be seen that, for the rise portions, the acceleration changes over the speed profile segments have the same magnitudes:

$$\Delta A_{concave} = A_{end} - A_{start} = A_{max} - 0 \tag{4.6}$$

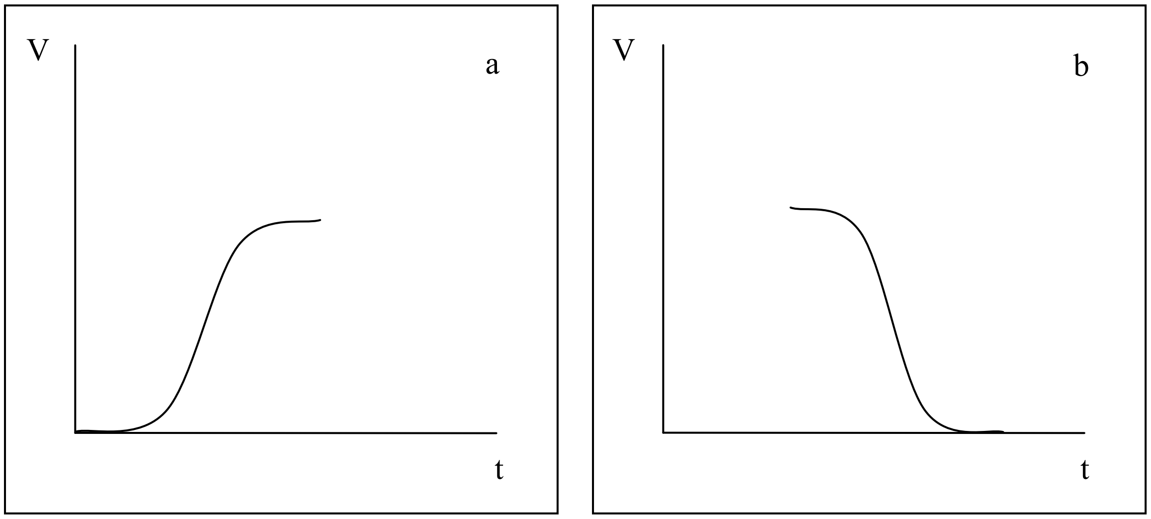

Figure 4.10. Perfect s-curve speed profiles.

$$\Delta A_{convex} = A_{end-}A_{start} = 0 - A_{max} \tag{4.7}$$

Dividing by their respective jerks it can be seen that

$$\Delta t_{concave} = A_{max} / J_0 = \Delta t_{convex} = -A_{max} / - J_0 \tag{4.8}$$

So the total time for the speed change is

$$T = 2A_{max} / J_0 \tag{4.9}$$

Plugging this into (4.2) and subtracting starting velocities yields

$$\Delta V_{concave} = \Delta V_{convex} = \frac{A_{max}^2}{2J_0} \tag{4.10}$$

so

$$\Delta V_{rise} = \frac{A_{max}^2}{J_0} \tag{4.11}$$

Plugging T into (4.1) and subtracting starting length yields

$$\Delta S_{concave} = \frac{V_{start} A_{max}}{J_0} + \frac{2A_{max}^3}{3J_0^2} \tag{4.12}$$

$$\Delta S_{convex} = \frac{(2V_{start} + \Delta V_{rise}) A_{max}}{2J_0} + \frac{A_{max}^3}{3J_0^2} \tag{4.13}$$

$$\Delta S_{rise} = \frac{2V_{start} A_{max}}{J_0} + \frac{A_{max}^3}{J_0^2} \tag{4.14}$$

where J_0 is equal to the maximum jerk for the move segment and ΔS is equal to the length of the move segment.

Similarly, for the fall portion

$$\Delta S_{fall} = \frac{2V_{start}A_{max}}{J_0} - \frac{A_{max}^3}{J_0^2} \tag{4.15}$$

V_{start} is also a constant. This yields a cubic equation in A_{max}. Solving (4.15) for real positive roots of A_{max} gives the useable ranges for A_{max}. Also excluded are solutions which lead to the case $\Delta V > V_{start}$. There are three possible cases:

a) One useable A_{max} value. Here the useable values for A_{max} are between zero and A_1 or, if the profile can reach zero speed before the end of the move, between zero and the value of A_{max} which satisfies $\Delta V = V_{start}$. There is one connected region of attainable speeds (Fig. 4.11).

b) Two useable A_{max} values. Here the useable values for A_{max} are between zero and A_1 and between A_2 and the value of A_{max} which satisfies $\Delta V = V_{start}$. There are two disconnected regions of attainable speeds (Fig. 4.12).

c) Three useable A_{max} values. Here the useable values for A_{max} are between zero and A_2 and between A_2 and A_3. There are two disconnected regions of attainable speeds (Fig. 4.13).

Observe that the accelerating case (4.14) does not have disconnected regions of attainable speeds since there is only one real positive solution for A_{max}. This can be shown by inspection since the coefficients of A_{max} are all positive, and the constant value is negative. Thus the equation intersects the abscissa exactly once. The useable values for A_{max} for the accelerating case are between zero and A_1.

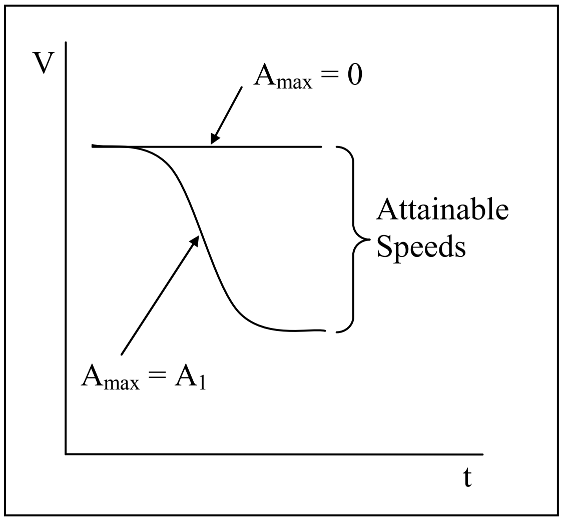

Figure 4.11. Illustration of attainable speed region for 1 useable A_{max} value.

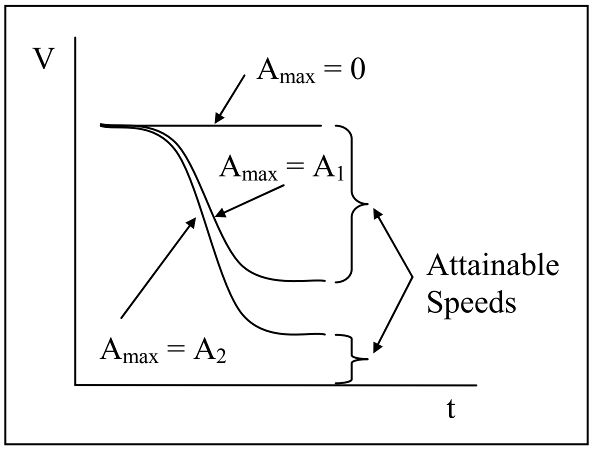

Figure 4.12. Illustration of attainable speed region for 2 useable A_{max} values.

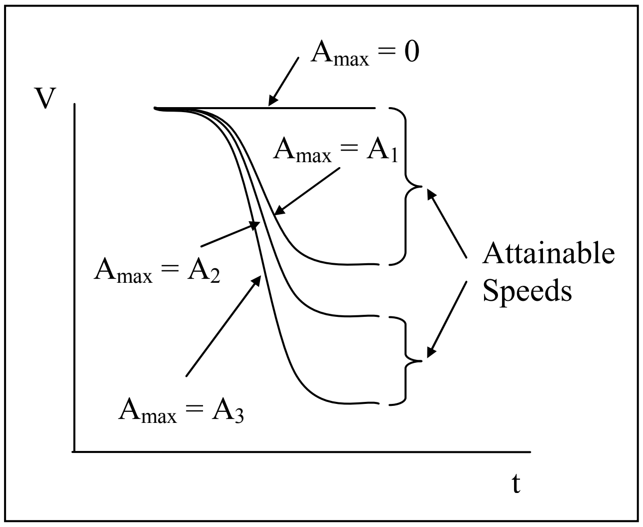

Figure 4.13. Illustration of attainable speed region for 3 useable A_{max} values.

5 METHOD: DYNAMICS

There are two types of dynamic limitations that arise in machining operations: process limitations and machine limitations. Process limitations are machine independent and relate only to motion along the path and interactions between the tool and the workpiece. For example, forces on a cutting tool depend upon the speed, acceleration, and jerk at which the tool is moved through material. Machine limitations apply to each joint of the machine tool and depend upon both the shape of the path and the motion along the path as defined by the speed profile. Due to this relationship, the path dynamics (speed, acceleration, jerk) that will give acceptable joint dynamics must be determined.

This chapter will outline a method for determining the allowable path dynamics for moves. The allowable values for path dynamics can then be used by the speed profiler in Chapter 4 to develop feasible speed profiles. Section 5.1 presents the mathematical relationship between motion along curves in path space and motion in joint space. Section 5.2 gives a quick overview of the variation diminishing property of Bezier curves. Section 5.3 presents a heuristic method for determining allowable speeds based on the variation diminishing property.

5.1 PATH-JOINT RELATIONSHIPS

A Bezier path is described by the equation

$$\mathbf{P}(u) = \sum_{i=0}^{n} \frac{v_i \mathbf{P}_i B_i^n(u)}{v_i B_i^n(u)} \tag{5.1}$$

where

$$\mathbf{P}_i = \begin{bmatrix} P_{ix} & P_{iy} & P_{iz} \end{bmatrix}^T \tag{5.2}$$

are points in Cartesian space,

$$B_i^n(u) = \begin{pmatrix} n \\ i \end{pmatrix} u^i (1-u)^{n-i} \tag{5.3}$$

are Bernstein polynomials,

$$\begin{pmatrix} n \\ i \end{pmatrix} = \frac{n!}{(n-i)!\,i!} \tag{5.4}$$

is the binomial coefficient, and v_i are positive definite weighting values.

Section 5.1.1 presents the equations for relating a curve and its parametric derivatives in path space to joint space. Section 5.1.2 presents the relations for derivatives with respect to arc length. Section 5.1.3 presents the relations for derivatives with respect to time.

5.1.1 PARAMETRIC DERIVATIVES

For 3-degree-of-freedom machines, such as those in Fig. 5.1, points in path space **P** can be related to points in joint space **q** by use of a machine-specific inverse kinematics transformation **K**, so that

$$\mathbf{q}(\mathrm{u}) = \mathbf{K}(\mathbf{P}(\mathrm{u})) \tag{5.5}$$

where

$$\mathbf{K}(\mathbf{P}) = \begin{bmatrix} q_1(\mathbf{P}) \\ \vdots \\ q_m(\mathbf{P}) \end{bmatrix} \tag{5.6}$$

While the inverse kinematics transformations for 3-axis mechanisms are relatively simple, the relationship between path dynamics and joint dynamics are a bit more complicated. These dynamics must be kept in check to ensure smooth motion along the path and stay within the capabilities of the machine.

Parametric relationships for joint dynamics can be found by taking the derivatives of (5.5):

$$\mathbf{q}'(\mathrm{u}) = \mathrm{d}\mathbf{K}(\mathbf{P}(\mathrm{u}))\mathbf{P}' \tag{5.7}$$

where

$$d\mathbf{K}(\mathbf{P}) = \begin{bmatrix} dq_1(\mathbf{P}) \\ \vdots \\ dq_m(\mathbf{P}) \end{bmatrix} = \begin{bmatrix} \frac{\partial q_1(\mathbf{P})}{\partial P_x} & \frac{\partial q_1(\mathbf{P})}{\partial P_y} & \frac{\partial q_1(\mathbf{P})}{\partial P_z} \\ \vdots & \vdots & \vdots \\ \frac{\partial q_m(\mathbf{P})}{\partial P_x} & \frac{\partial q_m(\mathbf{P})}{\partial P_y} & \frac{\partial q_m(\mathbf{P})}{\partial P_z} \end{bmatrix} = \frac{\partial q_i(\mathbf{P})}{\partial P_j} \tag{5.8}$$

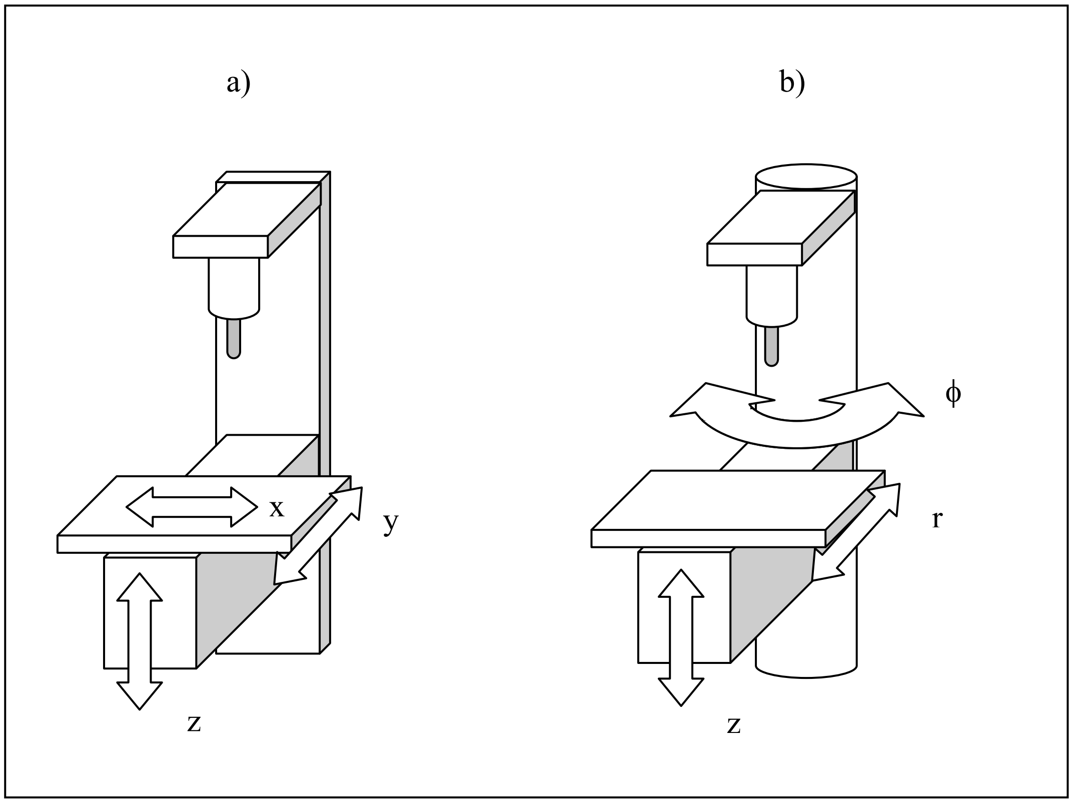

Figure 5.1. Some simple 3-axis mechanisms. a) Rectangular mechanism. b) Cylindrical mechanism.

Similarly,

$$\mathbf{q}''(u) = \left(d^2\mathbf{K}(\mathbf{P}(u))(\mathbf{P}')\right)(\mathbf{P}') + d\mathbf{K}(\mathbf{P}(u))\mathbf{P}'' \tag{5.9}$$

$$\mathbf{q}'''(\mathrm{u}) = \left(\left(\mathrm{d}^3\mathbf{K}(\mathbf{P}(\mathrm{u}))(\mathbf{P}')\right)(\mathbf{P}')\right)(\mathbf{P}') + 3\left(\mathrm{d}^2\mathbf{K}(\mathbf{P}(\mathrm{u}))(\mathbf{P}')\right)(\mathbf{P}'') + \mathrm{d}\mathbf{K}(\mathbf{P}(\mathrm{u}))\mathbf{P}''' \qquad (5.10)$$

where

$$\mathrm{d}^2\mathbf{K}(\mathbf{P}) = \frac{\partial^2 \mathrm{q_i}(\mathbf{P})}{\partial \mathrm{P_j} \partial \mathrm{P_k}} \quad \text{(a 3-dimensional tensor)} \qquad (5.11)$$

$$\mathrm{d}^3\mathbf{K}(\mathbf{P}) = \frac{\partial^3 \mathrm{q_i}(\mathbf{P})}{\partial \mathrm{P_j} \partial \mathrm{P_k} \partial \mathrm{P_l}} \quad \text{(a 4-dimensional tensor)} \qquad (5.12)$$

5.1.2 ARC-LENGTH DERIVATIVES

Using the parametric joint derivatives, the derivatives with respect to arc-length can be calculated.

$$\mathbf{q}_\mathrm{S}(\mathrm{u}) = \frac{\mathrm{d}\mathbf{q}(\mathrm{u})}{\mathrm{dS}} = \mathbf{q}'(\mathrm{u})\mathrm{u_S} \qquad (5.13)$$

where

$$\mathrm{u_S} = \frac{1}{|\mathbf{q}'(\mathrm{u})|} \qquad (5.14)$$

and

$$\mathbf{q}_{SS}(u) = \mathbf{q}''(u)u_S^2 + \mathbf{q}'(u)u_S \frac{du_s}{du} \tag{5.15}$$

$$\mathbf{q}_{SSS}(u) = \mathbf{q}'''(u)u_S^3 + 3\mathbf{q}''(u)u_S^2 \frac{du_S}{du} + \mathbf{q}'(u)\left(u_S\left(\frac{du_S}{du}\right)^2 + u_S^2 \frac{d^2u_S}{du^2} \right) \tag{5.16}$$

5.1.3 TIME DERIVATIVES

The time derivatives are calculated from the arc-length derivatives as follows:

$$\dot{\mathbf{q}}(u) = \frac{d\mathbf{q}(u)}{dt} = \mathbf{q}_S(u)\frac{dS}{dt} \tag{5.17}$$

Note that the final term in (5.17) is simply a speed term, so (5.17) can be written a little more clearly as

$$\dot{\mathbf{q}}(u) = \mathbf{q}_S(u)V \tag{5.18}$$

Continuing with the next two derivatives,

$$\ddot{\mathbf{q}}(u) = \mathbf{q}_{SS}(u)V^2 + \mathbf{q}_S(u)A \tag{5.19}$$

$$\dddot{\mathbf{q}}(u) = \mathbf{q}_{SSS}(u)V^3 + 3\mathbf{q}_{SS}(u)AV + \mathbf{q}_S(u)J \tag{5.20}$$

Equations 5.18 - 5.20 map the relationship between the path dynamics and joint dynamics. The left-hand terms are the machine joint dynamics and are known. Inserting their maximum values and inverting the equations yields a method for calculating the allowable path dynamics:

$$V_{max} = \min(|\mathbf{V}|) \tag{5.21}$$

where

$$\mathbf{V} = \frac{\dot{\mathbf{q}}(u)}{\mathbf{q}_S(u)} \tag{5.22}$$

and the division of two vectors is a component-wise division.

Likewise,

$$A_{max} = \min(|\mathbf{A}|) \tag{5.23}$$

$$\mathbf{A} = \frac{\ddot{\mathbf{q}}(u) - \mathbf{q}_{SS}(u)V^2}{\mathbf{q}_S(u)} \qquad -V_{max} \le V \le V_{max} \tag{5.24}$$

$$J_{max} = \min(|\mathbf{J}|) \tag{5.25}$$

$$\mathbf{J} = \frac{\ddot{\mathbf{q}}(u) - \mathbf{q}_{SSS}(u)V^3 - 3\mathbf{q}_{SS}(u)AV}{\mathbf{q}_S(u)} \tag{5.26}$$

where

$-V_{max} \le V \le V_{max}$

and

$-A_{max} \le A \le A_{max}$.

Calculating the extrema of these dynamic equations is expensive. Fortunately, the variation diminishing property (Section 5.2) of Bezier curves and a bit of heuristics can be used to make the job easier.

5.2 VARIATION DIMINISHING

The variation diminishing property of Beziers is that a line (for planar Beziers) or a plane (for 3D Beziers) will not intersect the curve more times than it intersects the control polygon. The physical meaning of this is that the curve will not "wiggle" more than the control polygon. This is illustrated in Fig. 5.2, where a variety of lines (dashed) are intersecting a Bezier curve and its control polygon. The solid line represents the Bezier curve. The dotted line represents the control polygon.

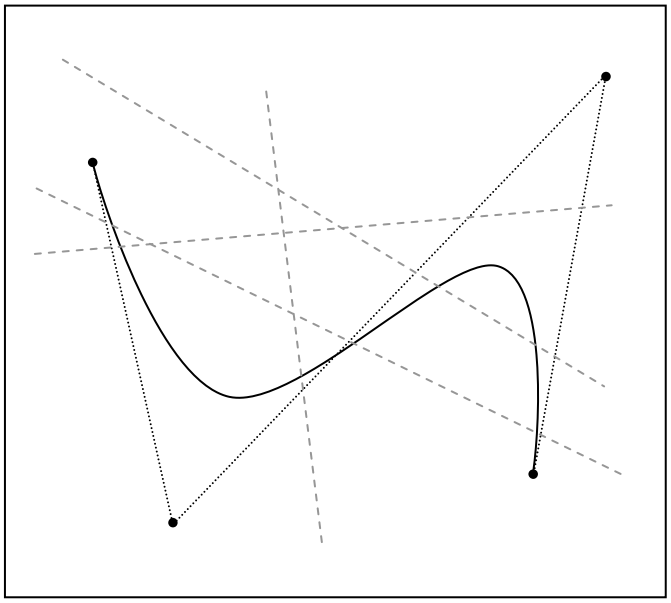

Figure 5.2. Illustration of variation diminishing property.

5.3 SAMPLING METHOD

Since the curve cannot wiggle more times than its control polygon, the variation of its shape is limited. If the curve is sampled at an appropriate interval, say $\Delta u = 0.1$, this variation will be evident. Fig. 5.3 gives an illustration of what such a sampling scheme would appear like when applied to a Bezier curve.

In addition to revealing the shape of a curve, the sampling method can be applied to the dynamic equations (5.22, 5.24, 5.26). A good approximation of the dynamics can be extracted by analyzing the dynamics equations at each of the sample points. From that a set of points on the curve is determined at which we know the limits on path dynamics. This information can be used in a number of ways. In this thesis, the simplest method is used, where the most conservative of the path dynamics is chosen and applied to the entire curve segment.

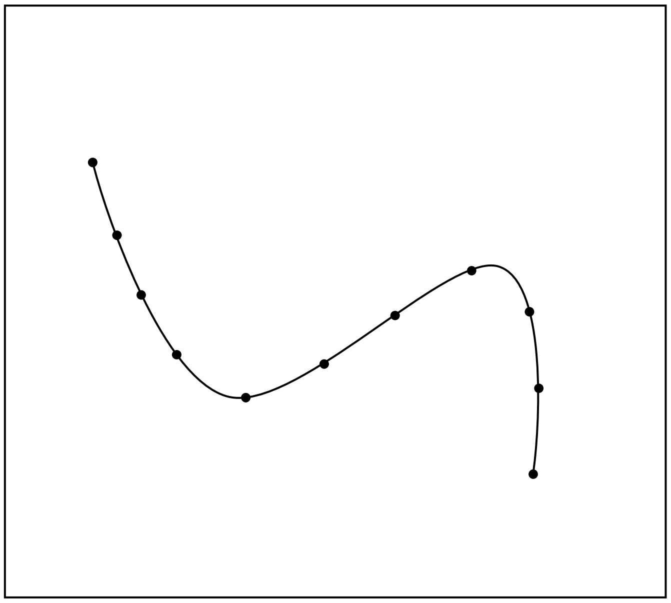
Figure 5.3. Illustration of sampling method.

6 RESULTS & DISCUSSION

This chapter presents the results of the methods developed in this thesis. The methods were tested under real-world conditions. The results are taken from the milling of the automotive surface shown in Fig. 6.1. The milling was done at BYU on a Tarus styling mill similar to the one shown in Fig. 6.2. Tool paths were generated using Unigraphics NX 2.0.

Section 6.1 presents the results of the Predictor-Corrector module for calculating appropriate parameter values. Section 6.2 gives the results of the Speed Profiling and Dynamics modules. Section 6.3 presents the machined part. Section 6.4 summarizes the results.

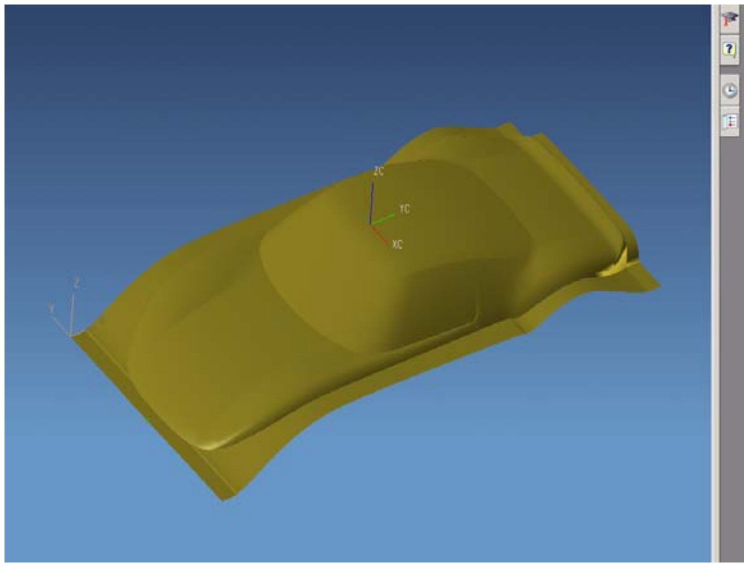

Figure 6.1. Automotive surfaces used for test.

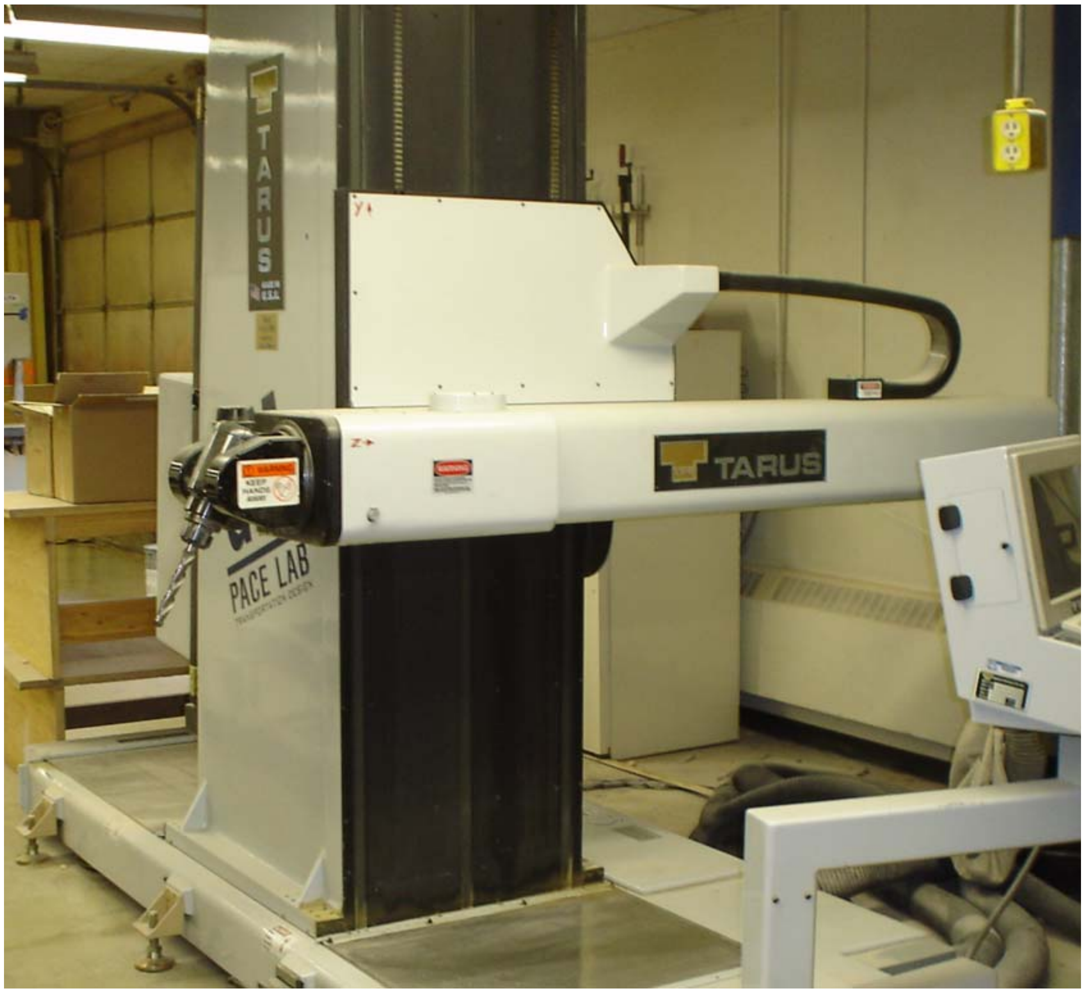

Figure 6.2. Tarus styling mill.

6.1 PREDICTOR-CORRECTOR

The job of the Predictor-Corrector is to evaluate the curve in a manner that will maintain the tool speed specified by the speed profiler. The Predictor-Corrector does this successfully when the speed error is kept below a specified level.

Fig. 6.3 shows a line plot of the speed error for the Predictor-Corrector for each step, normalized to the specified maximum error fraction of 1E^{-6}. Note that all values are below one. Thus the specified error fraction is being held by the Predictor-Corrector.

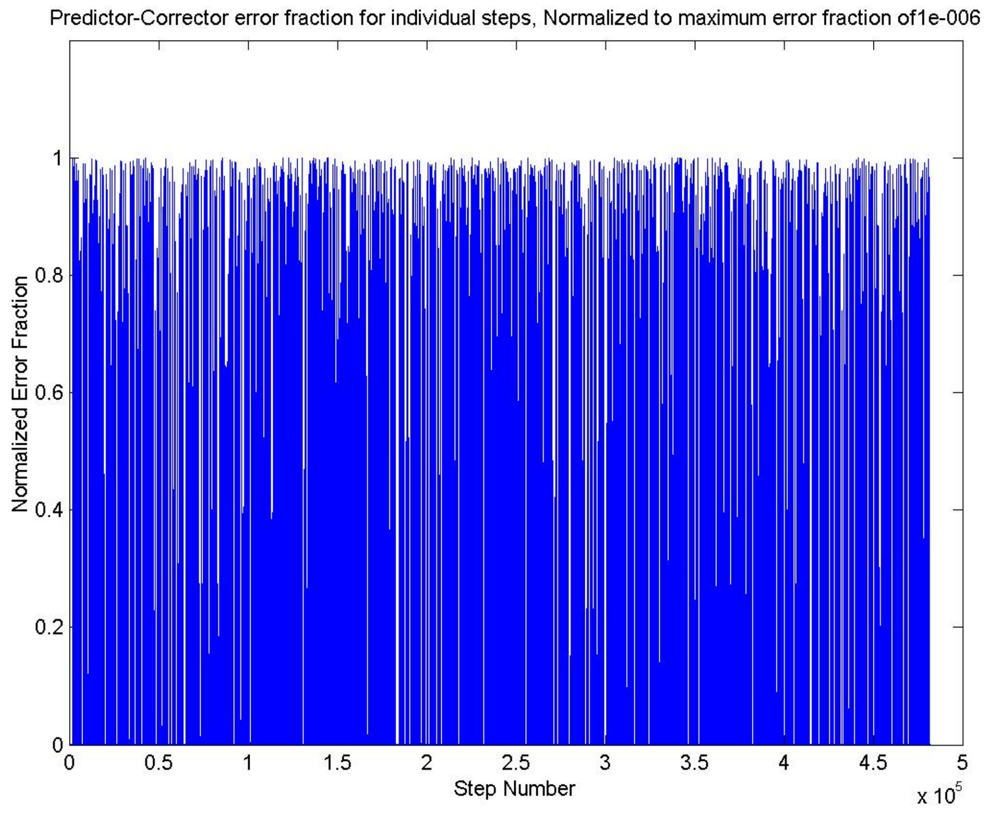

Figure 6.3. Predictor-Corrector error fraction for each step, normalized to the maximum allowable error fraction.

6.2 SPEED PROFILING AND MOTION DYNAMICS

The Motion Dynamics module analyzes each curve and decides the maximum allowable path speeds, accels, and jerks along that curve based on dynamic joint limitations and chordal error. The speed profiler keeps the speed as close to the desired speed as possible without violating motion dynamics.

The Speed Profiling and Motion Dynamics modules are closely related, so they are both evaluated at the same time.

Section 6.2.1 specifically evaluates the accuracy of the Speed Profiling module by examining the tool speed along the path. Section 6.2.2 analyzes the chordal error generated by the motion along the curve. Section 6.2.3 analyzes the dynamics of motion of each of the joints on the Tarus mill.

6.2.1 TOOL SPEED

The allowable speed is decided by the Motion Dynamics module and is different for each curve section. Fig 6.4 shows a line plot of the tool speed at each step, normalized to the allowable speed. All values are at or below one. This means that the allowable speed settings are being obeyed by the Speed Profiler.

It is interesting to note that, due to dynamic limitations, the speed profiler is not always able to hold the desired speed. This does not mean that the speed profiler is failing, simply that it is reducing speed at certain points in order to obey dynamic limitations. Fig. 6.5 shows a line plot of the actual tool speed at each step, normalized to the desired speed of 80 mm/s.

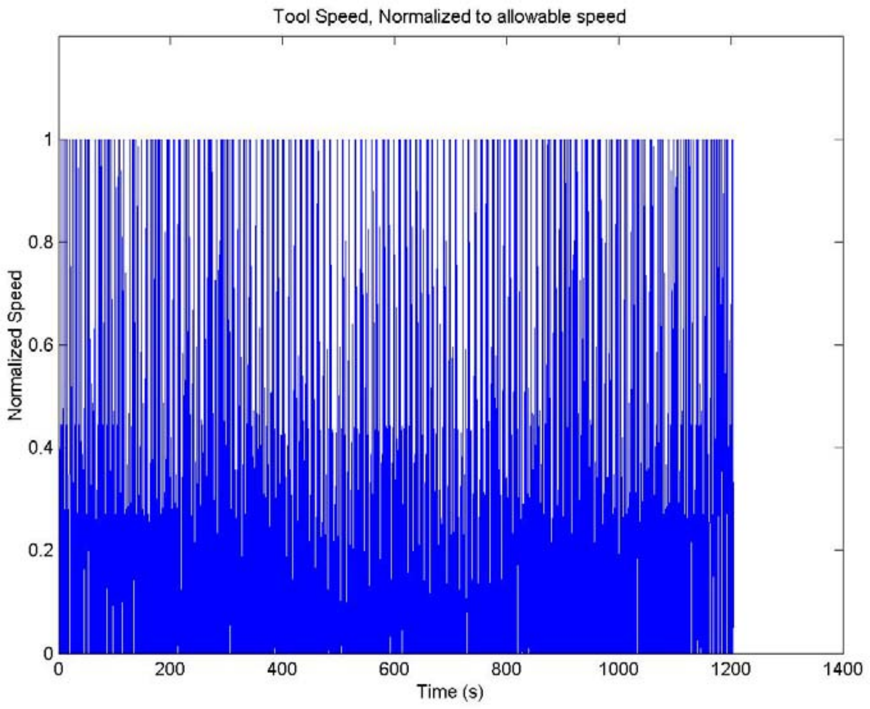

Figure 6.4. Tool speed, normalized to the allowable speed for each curve segment.

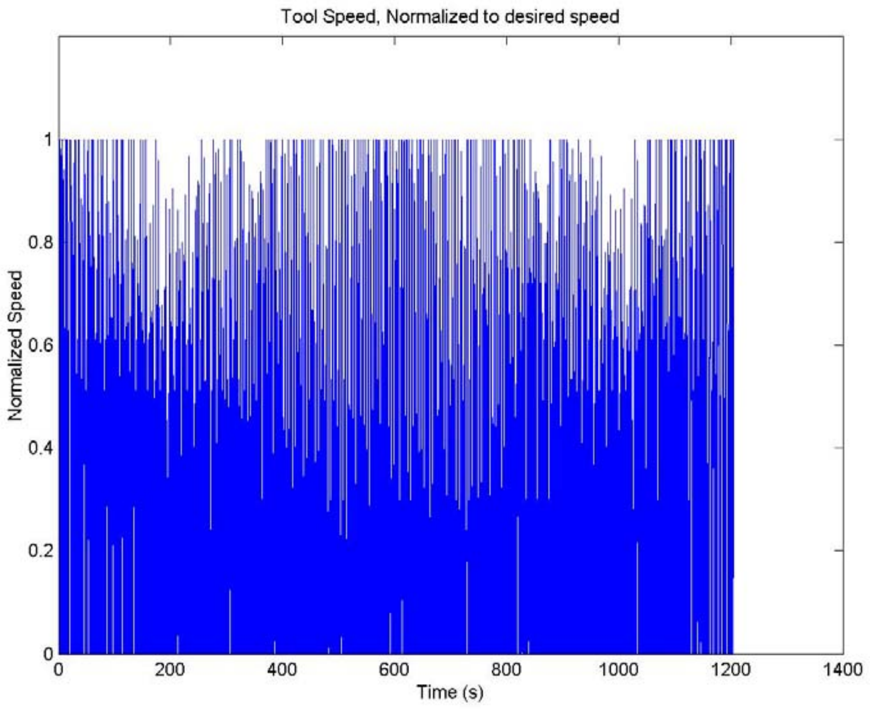

Figure 6.5. Tool speed, normalized to desired speed.

Figs. 6.6 to 6.18 show the behavior of the speed profiler at a more localized level. Fig. 6.6 shows the speed profile for the first sixteen seconds of the process plan. The actual tool speed is shown in blue, the commanded tool speed in green, and the maximum allowable tool speed for each move is shown in red. Fig. 6.7 shows the speed profile for the first four seconds of the process plan, with the same color scheme as in Fig. 6.6. Figs. 6.8 and 6.9 show the corresponding path acceleration and jerk profiles, respectively, with the actual value shown in blue and the allowable values shown in red and green. Note that the speed profiler attempts to reach and maintain the desired speed while respecting the maximum allowable speed, acceleration, and jerk. For reference, Figs. 6.10 to 6.18 show the resulting dynamics effects on the individual axes.

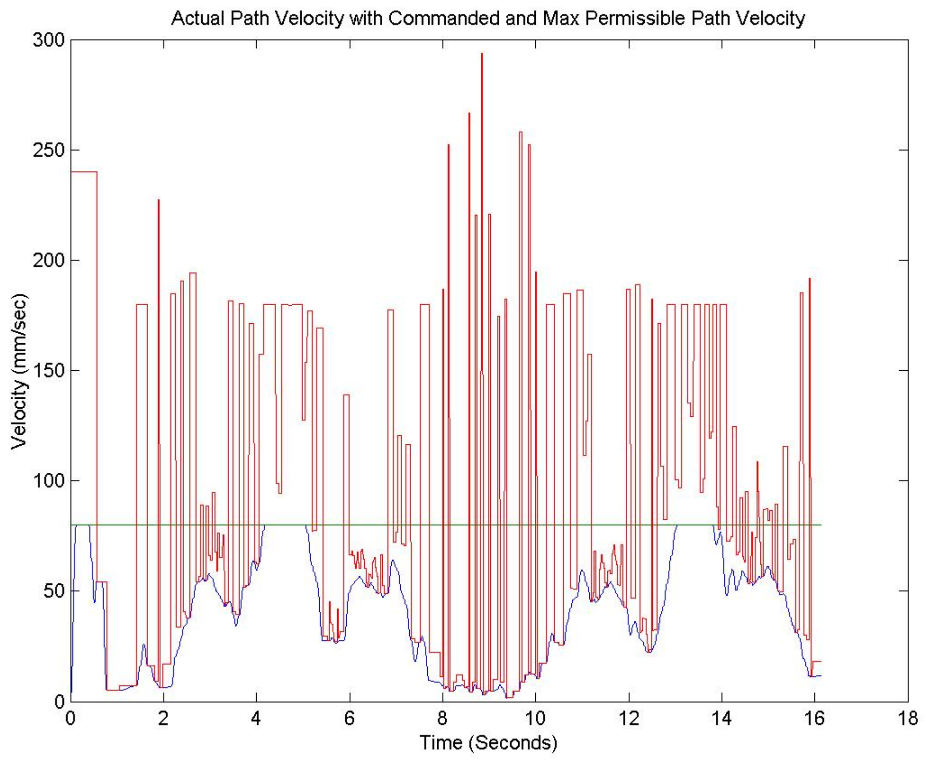

Figure 6.6. Tool speed with commanded and maximum allowable speed for first sixteen seconds of the milling process.

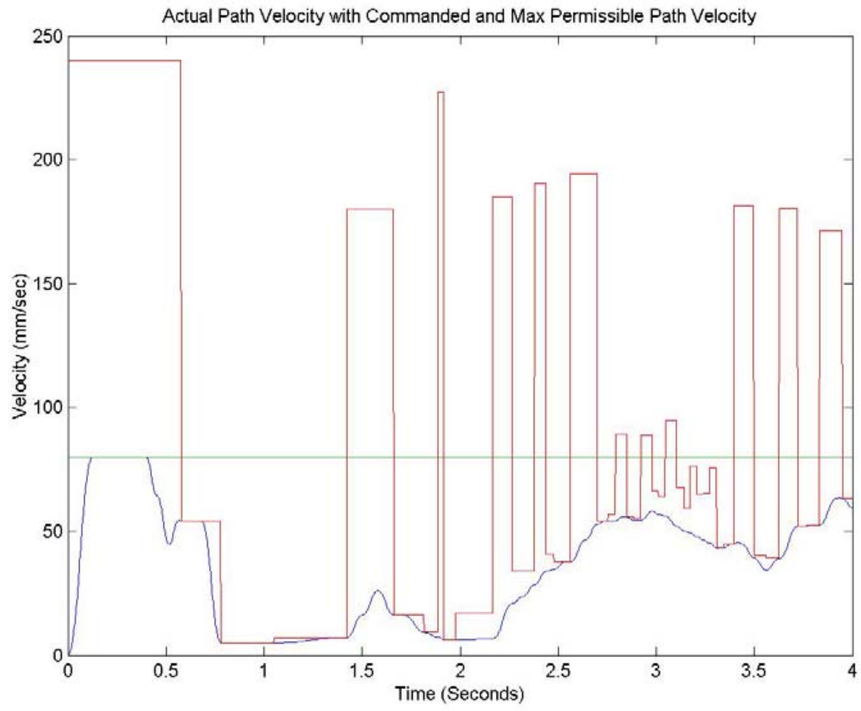

Figure 6.7. Tool speed with commanded and maximum allowable speed for first four seconds of the milling process.

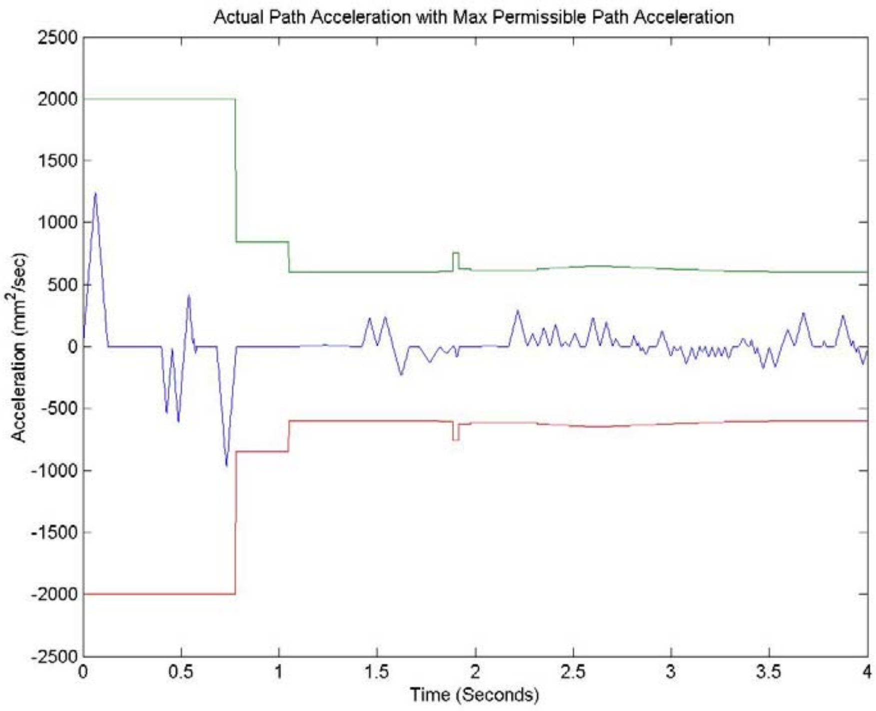

Figure 6.8. Tool acceleration with maximum allowable acceleration for first four seconds of the milling process.

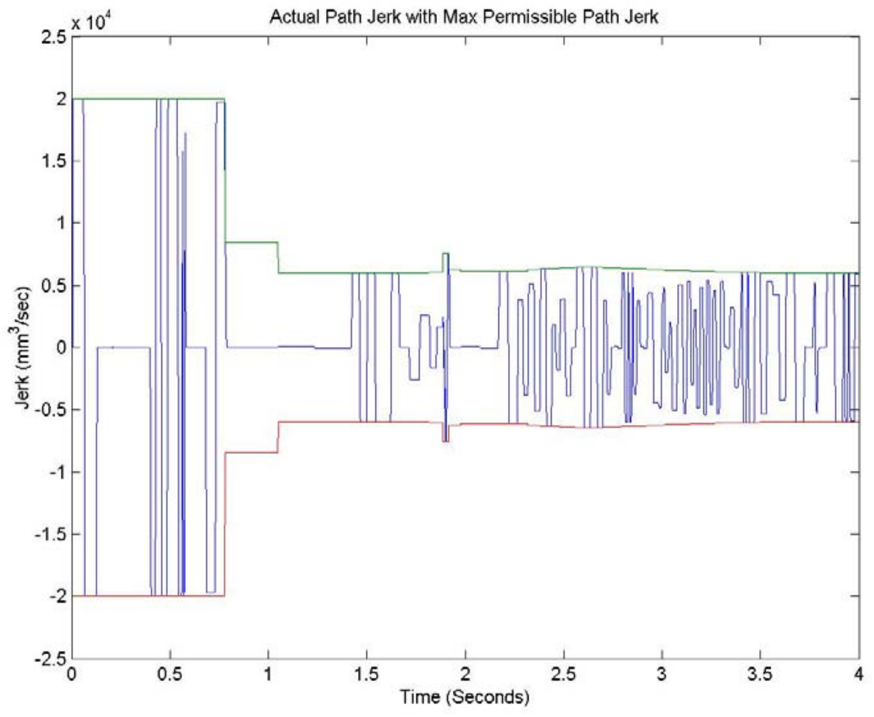

Figure 6.9. Tool jerk with maximum allowable jerk for first four seconds of the milling process.

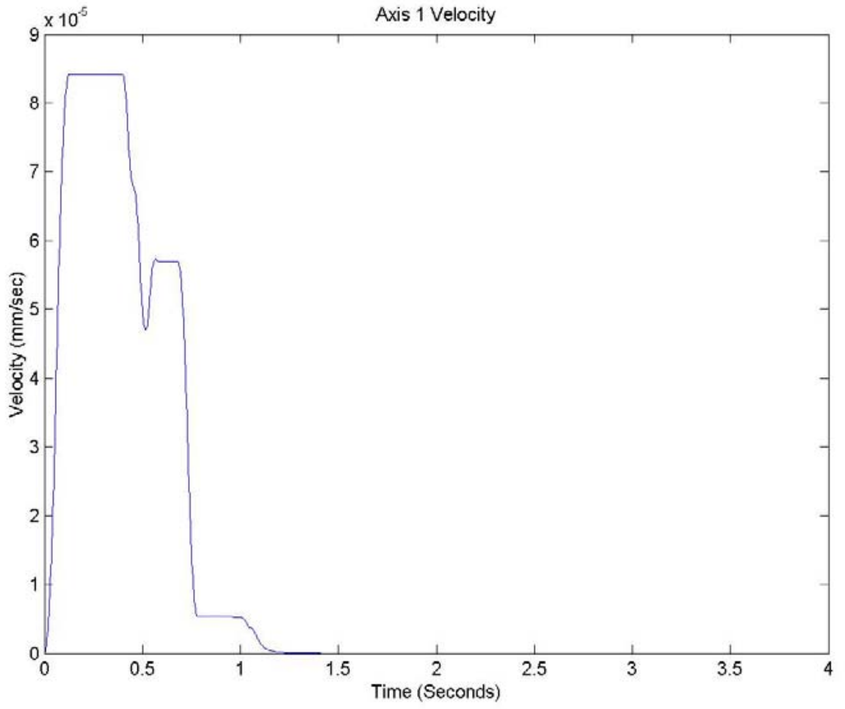

Figure 6.10. X axis velocity for first four seconds of the milling process.

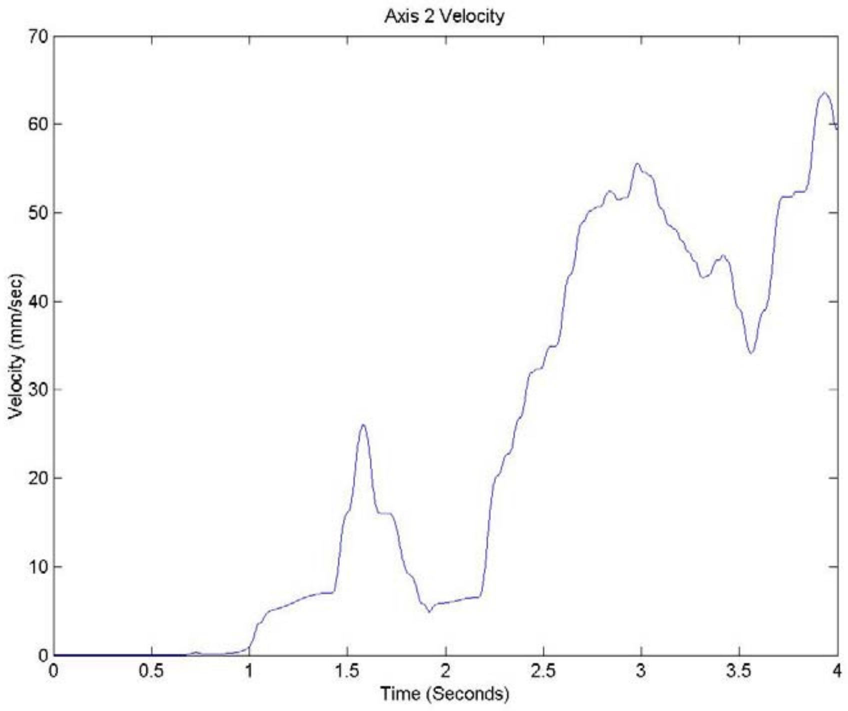

Figure 6.11. Y axis velocity for first four seconds of the milling process.

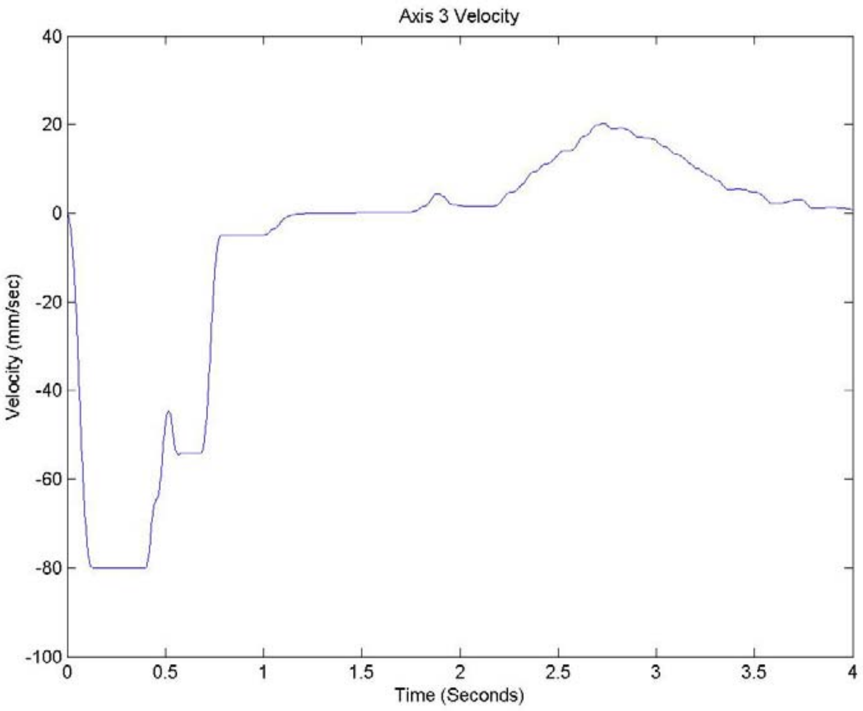

Figure 6.12. Z axis velocity for first four seconds of the milling process.

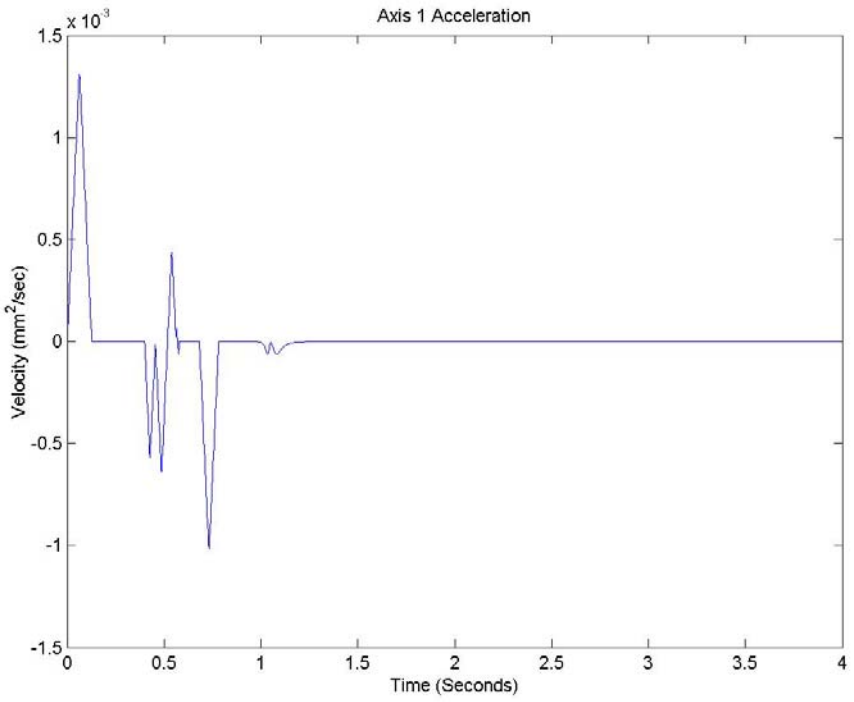

Figure 6.13. X axis acceleration for first four seconds of the milling process.

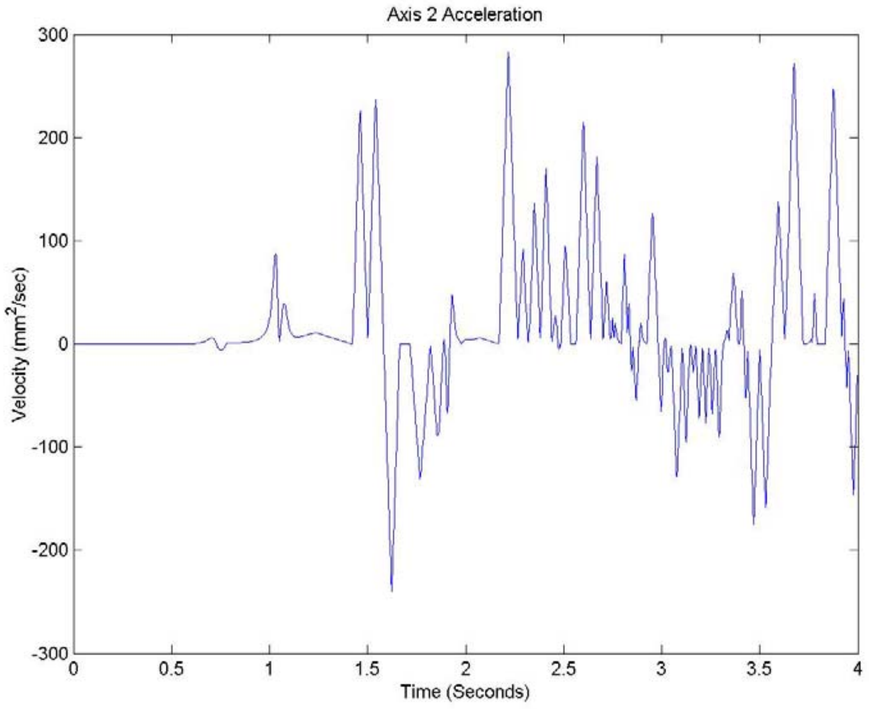

Figure 6.14. Y axis acceleration for first four seconds of the milling process.

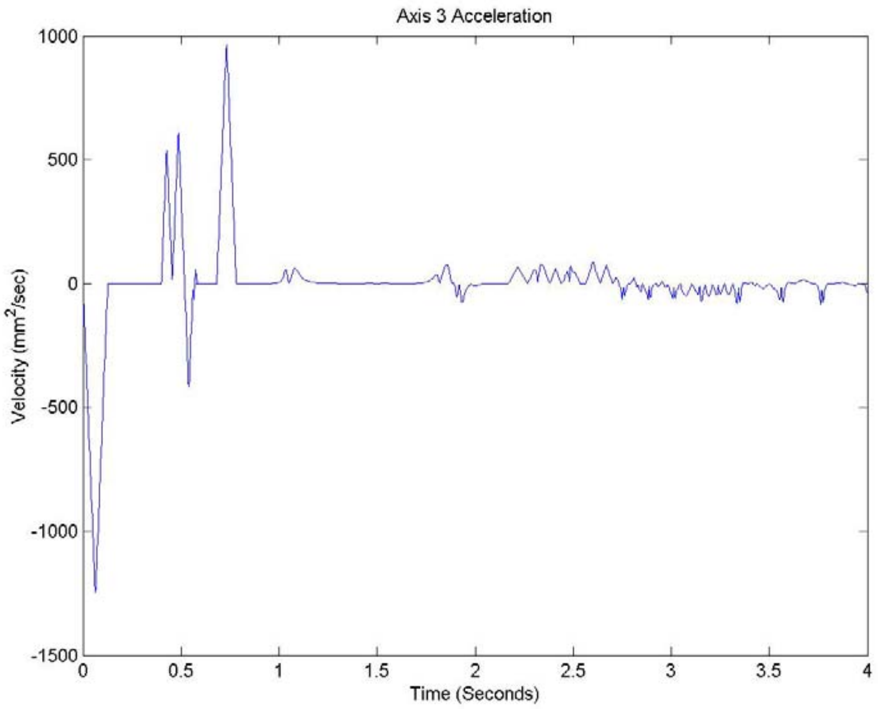

Figure 6.15. Z axis acceleration for first four seconds of the milling process.

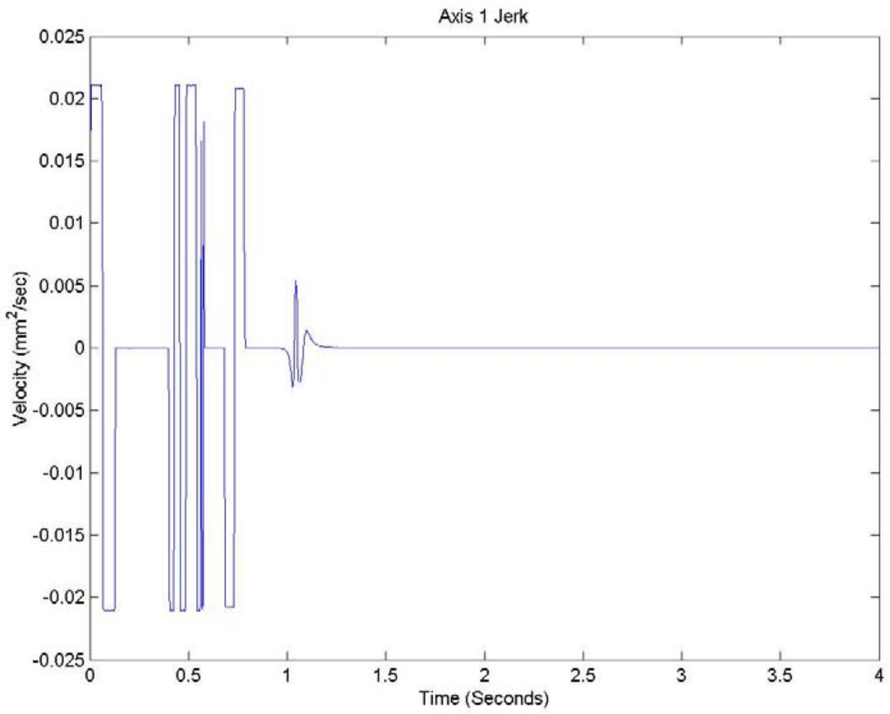

Figure 6.16. X axis jerk for first four seconds of the milling process.

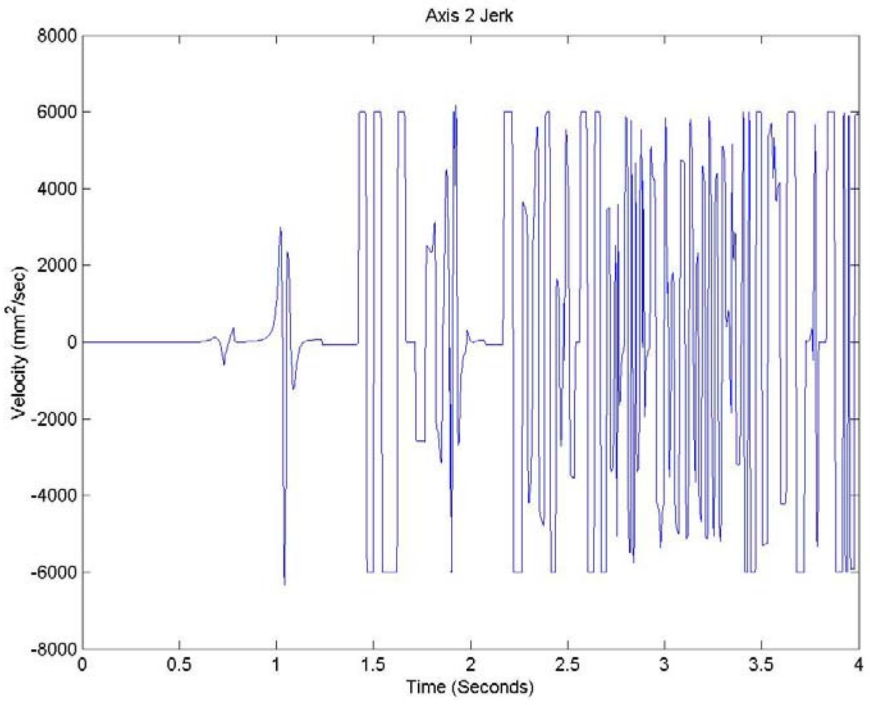

Figure 6.17. Y axis jerk for first four seconds of the milling process.

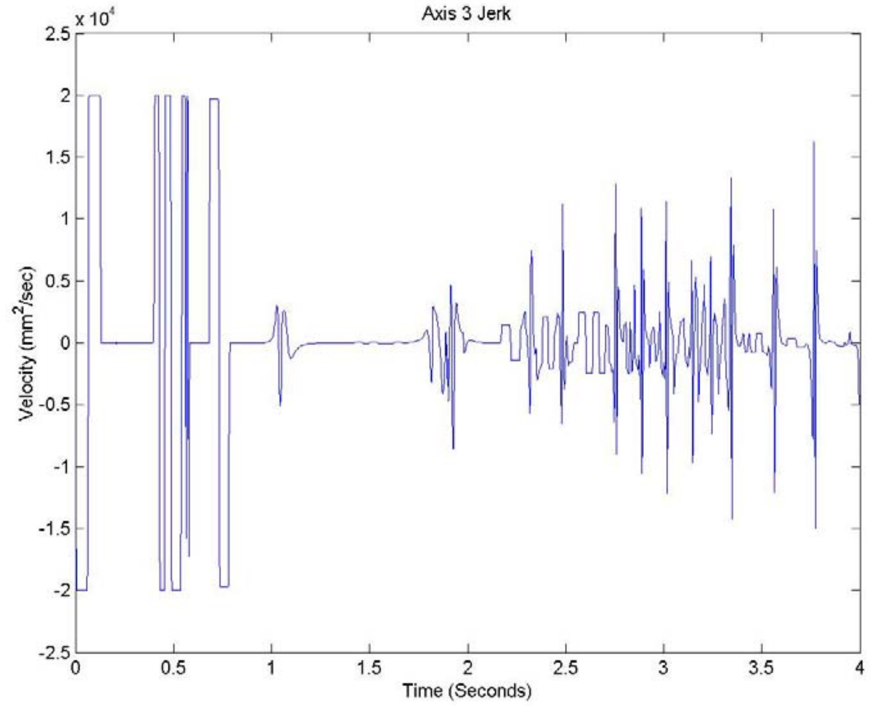

Figure 6.18. Z axis jerk for first four seconds of the milling process.

6.2.2 CHORDAL ERROR

Chordal error is the maximum distance between the curve geometry and the straight lines generated by digital control. Fig. 6.19 shows a line plot of the maximum chordal error for each step, normalized to the maximum allowable chordal error of 0.001 in. This plot shows that the chordal error is not of much concern in the present process plan, as all values are well below one.

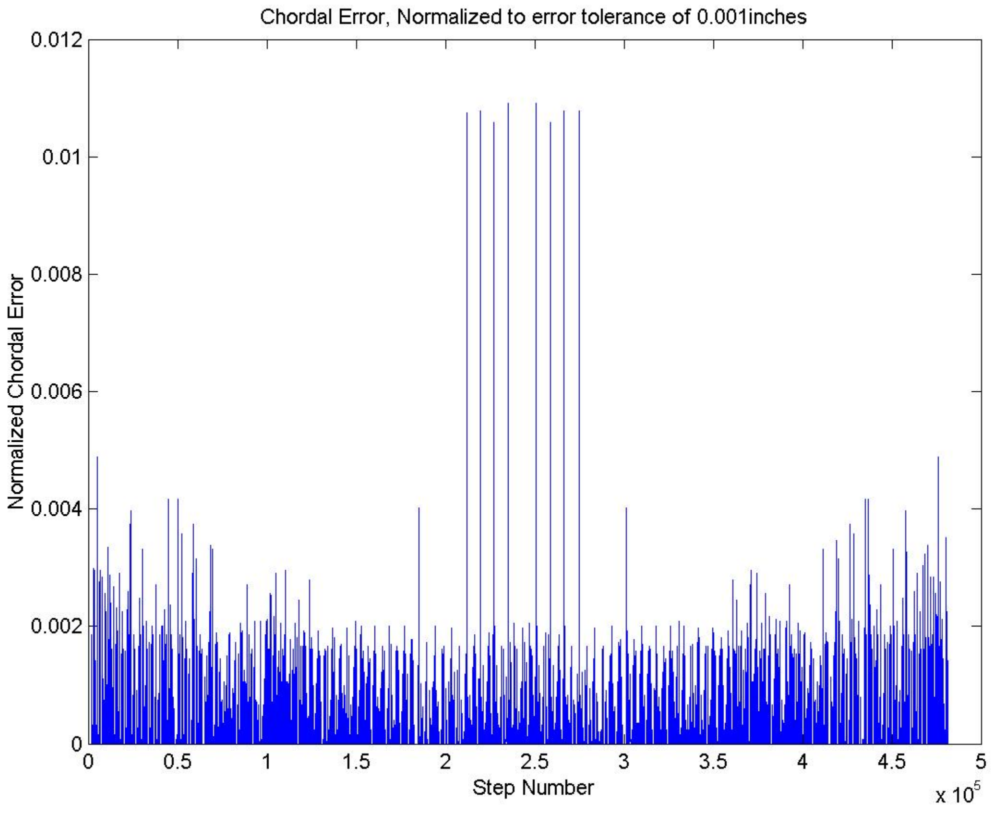

Figure 6.19. Chordal error, normalized to maximum error tolerance.

6.2.3 MOTION DYNAMICS

The motion dynamics for each axis on the Tarus styling mill are shown in Sections 6.2.3.1 to 6.2.3.4. The line plots shown in these sections have been normalized to their maximum allowable values. The maximum allowable values for each axis are shown in Table 6.1.

Table 6.1. Allowable axis dynamics for Tarus styling mill.

AXIS	**Speed (mm/s)**	**Accel (mm/s^2)**	**Jerk (mm/s^3)**
X	170	400	4000
Y	180	600	6000
Z	240	2000	20000

Section 6.2.3.1 gives the position plots for each axis. This is for reference purposes only. Section 6.2.3.2 gives the normalized speed plots for each axis. Section 6.2.3.3 gives the normalized speed acceleration plots for each axis. Section 6.2.3.4 gives the normalized jerk plots for each axis. Section 6.2.3.5 presents an analysis of the dynamic plots.

6.2.3.1 AXIS POSITIONS

This section presents the position verses time for each axis of the Tarus styling mill. These are provided for reference purposes and do not indicate the performance of the algorithms in this thesis.

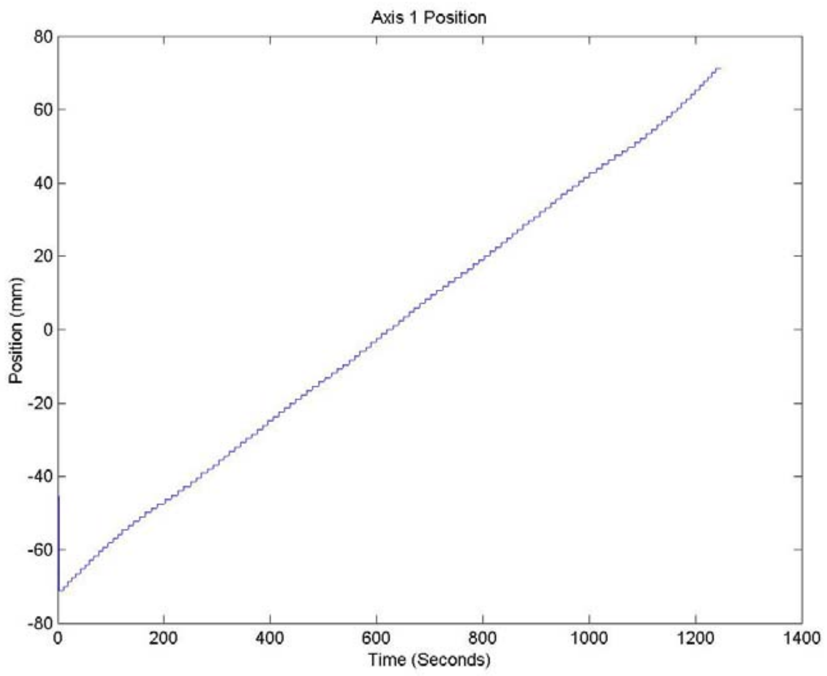

Figure 6.20. Dynamic position plot for X axis.

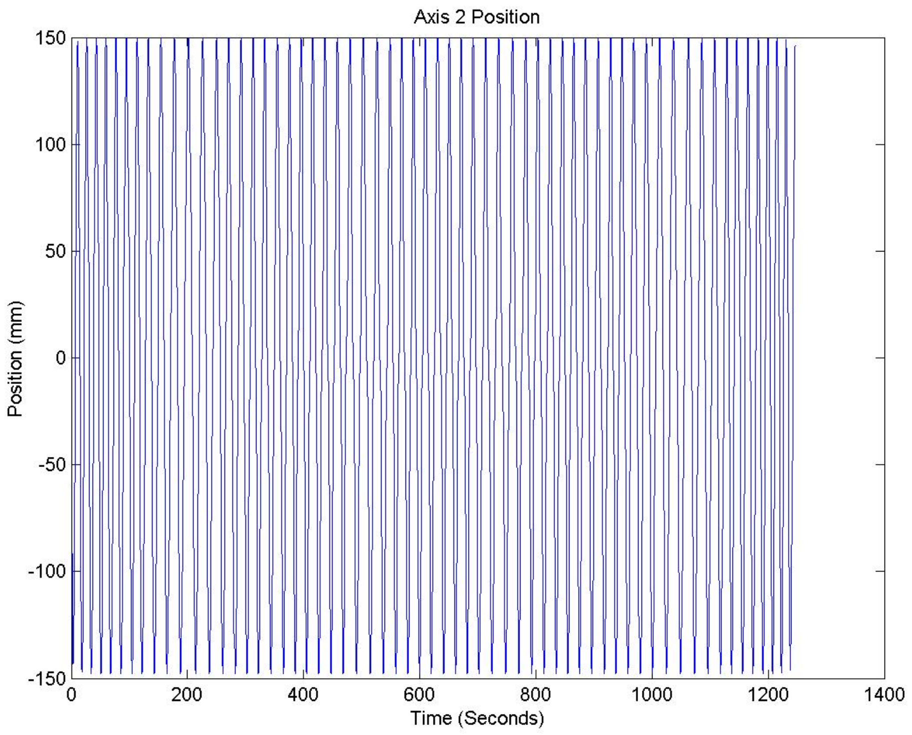

Figure 6.21. Dynamic position plot for Y axis.

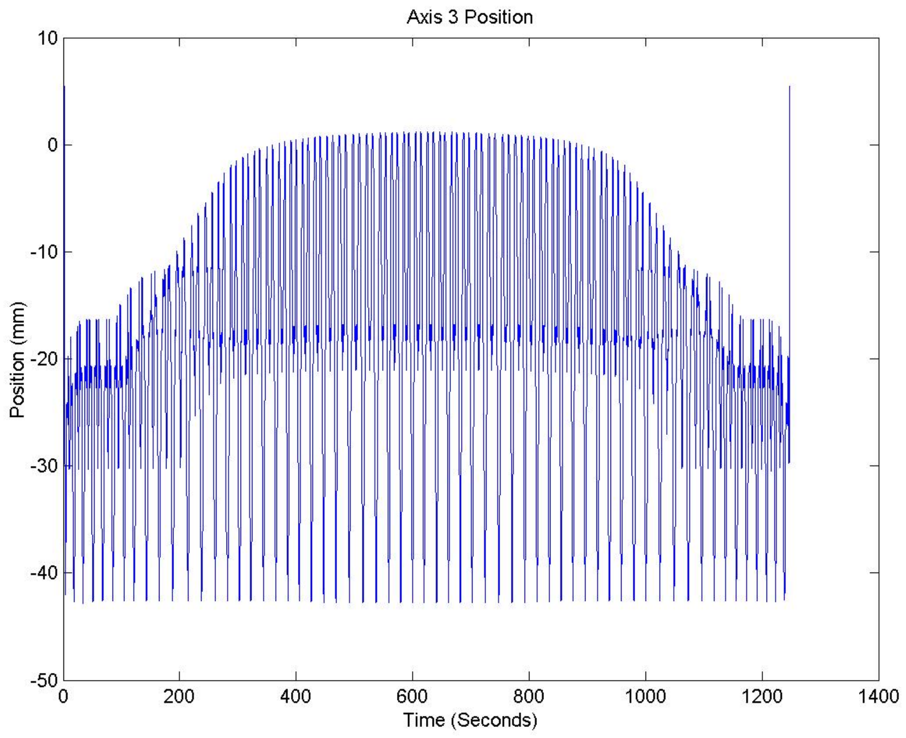

Figure 6.22. Dynamic position plot for Z axis.

6.2.3.2 NORMALIZED AXIS VELOCITIES

This section presents line plots of the normalized velocity verses time for each axis of the Tarus styling mill. It can be observed that all the absolute values are less than unity and thus the velocity limitations of each joint are being obeyed.

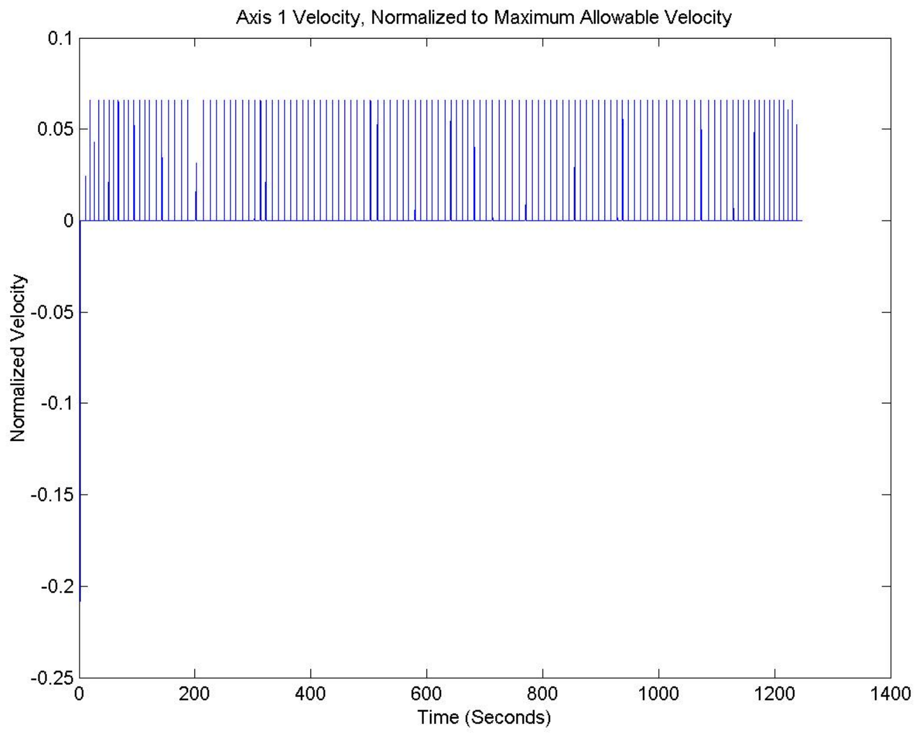

Figure 6.23. Dynamic velocity plot for X axis.

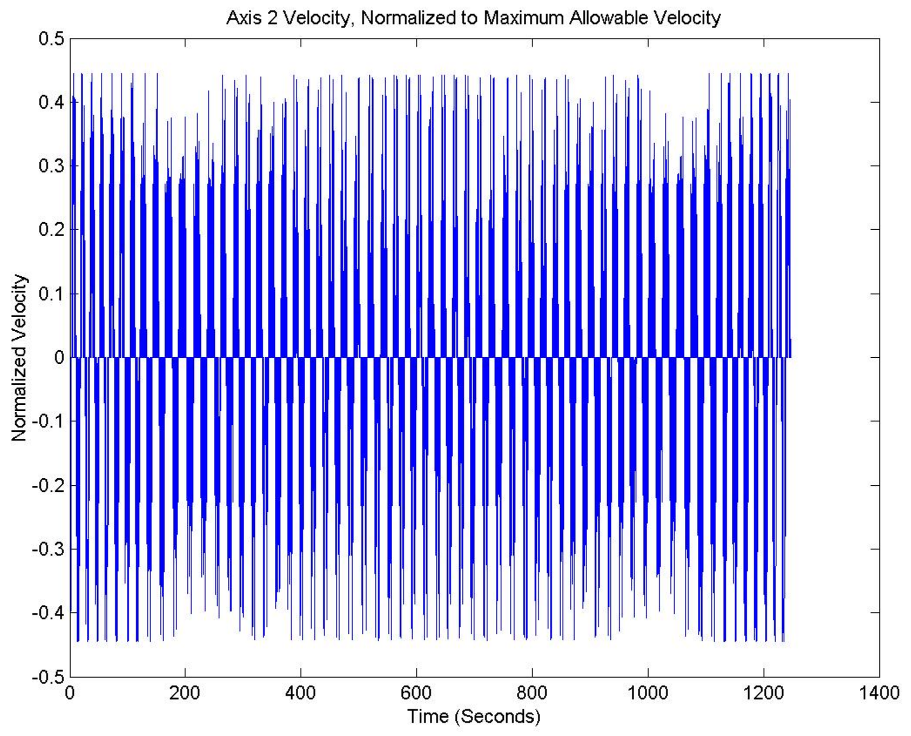

Figure 6.24. Dynamic velocity plot for Y axis.

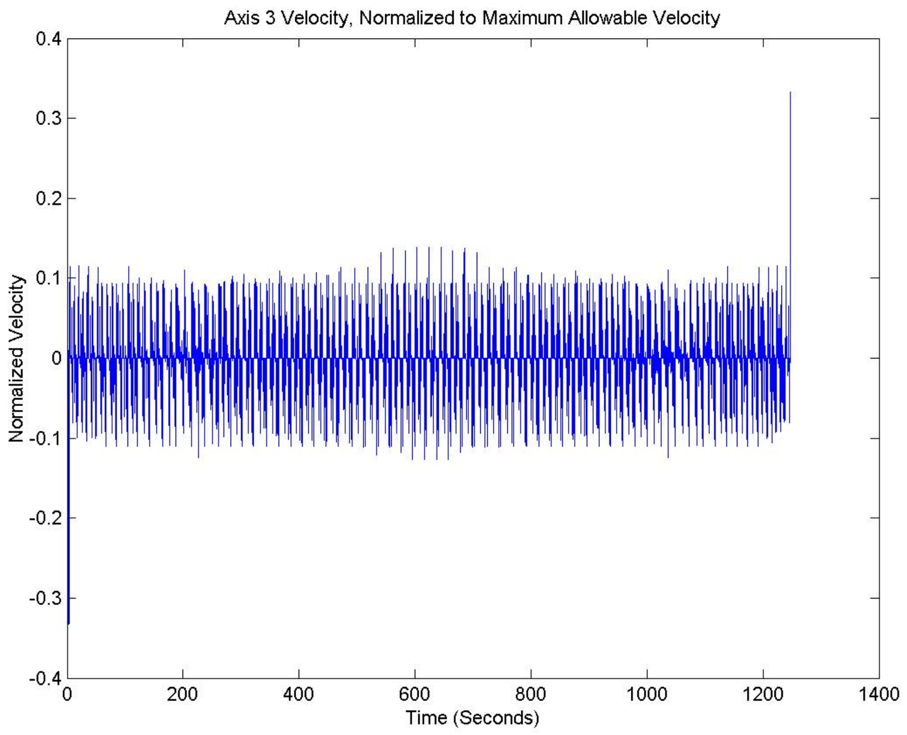

Figure 6.25. Dynamic velocity plot for Z axis.

6.2.3.3 NORMALIZED AXIS ACCELERATIONS

This section presents line plots of the normalized acceleration verses time for each axis of the Tarus styling mill. It can be observed that all the absolute values are less than unity and thus the acceleration limitations of each joint are being obeyed.

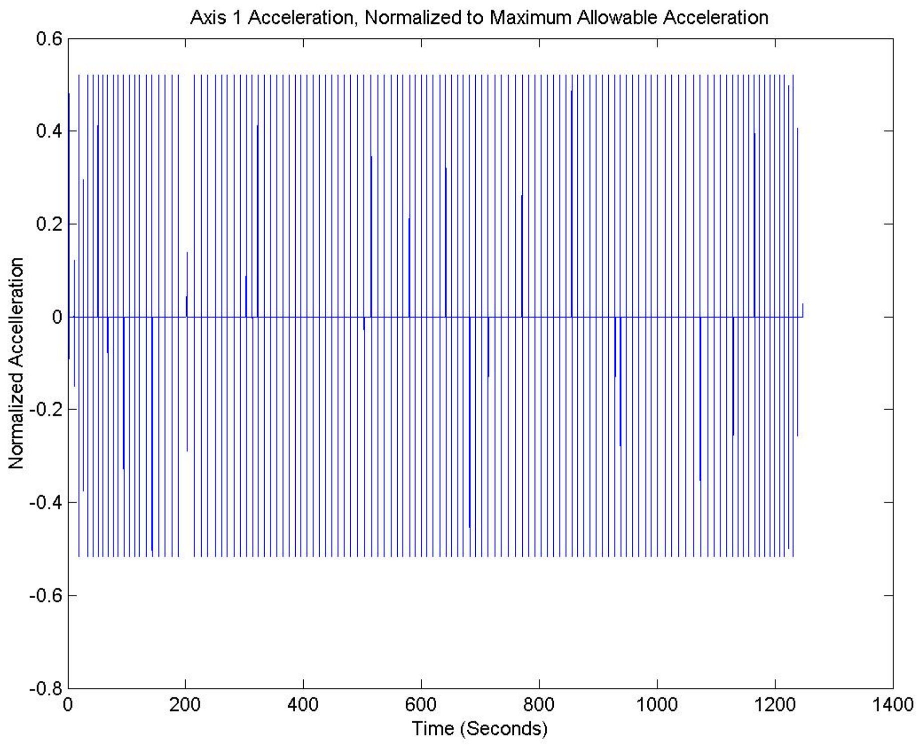

Figure 6.26. Dynamic acceleration plot for X axis.

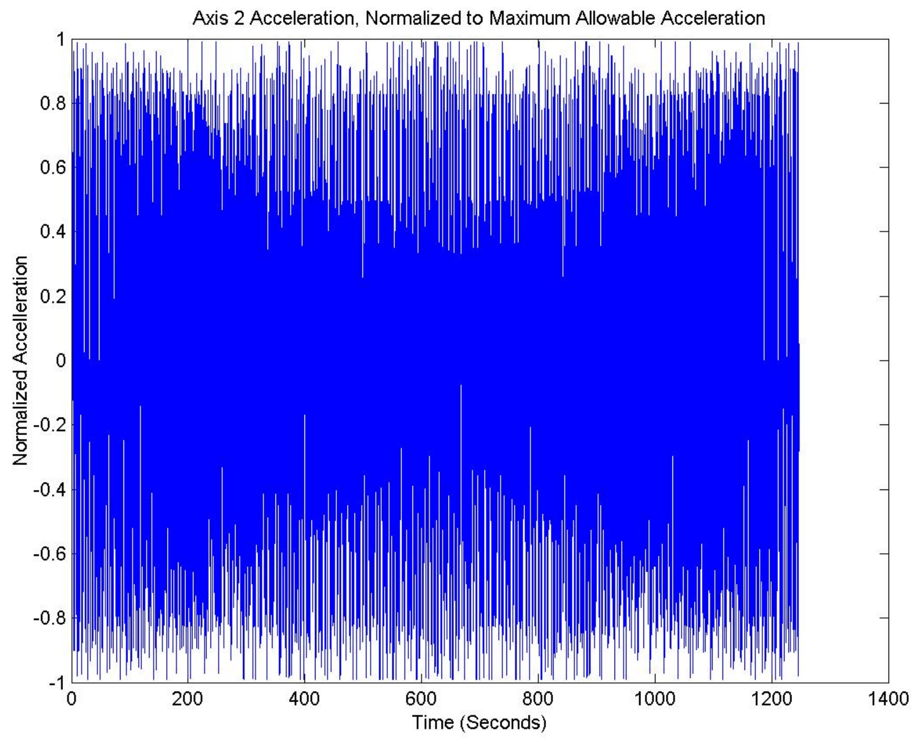

Figure 6.27. Dynamic acceleration plot for Y axis.

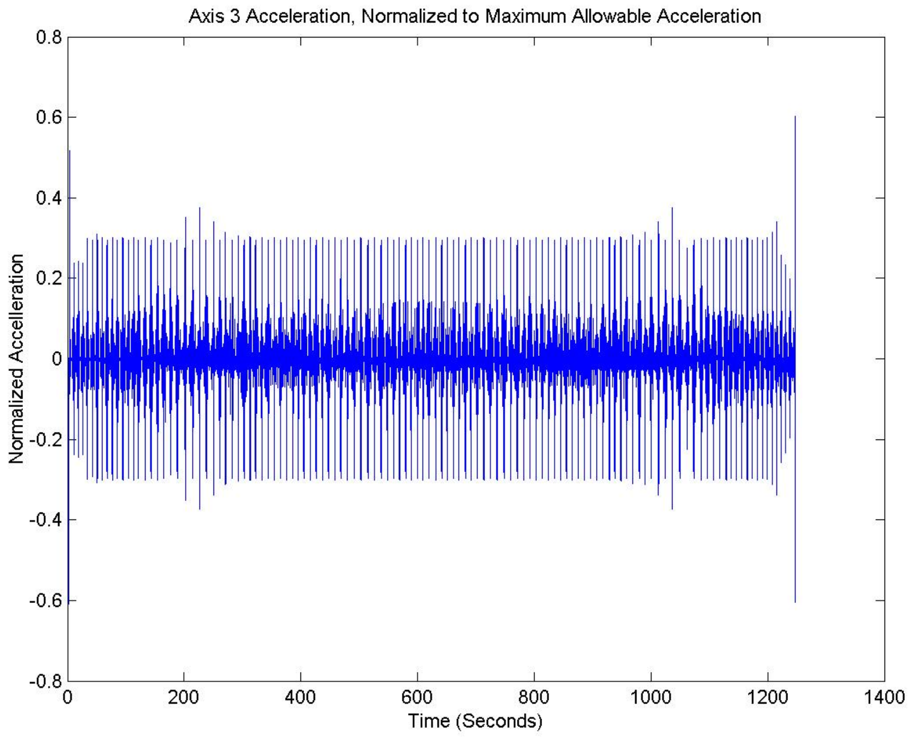

Figure 6.28. Dynamic acceleration plot for Z axis.

6.2.3.4 NORMALIZED AXIS JERKS

This section presents line plots of the normalized jerk verses time for each axis of the Tarus styling mill.

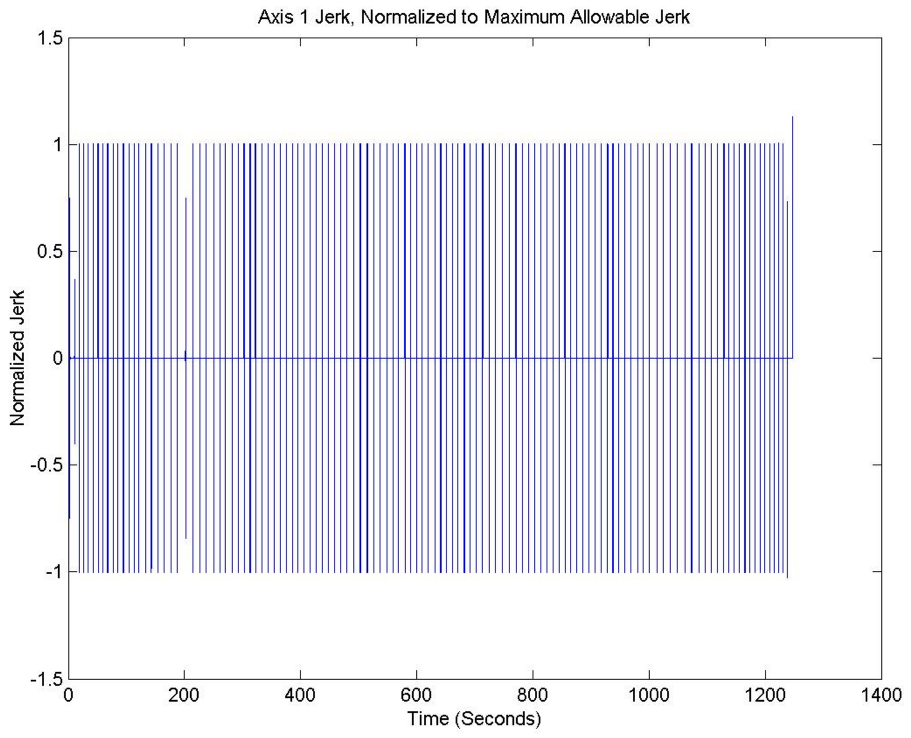

Figure 6.29. Dynamic jerk plot for X axis.

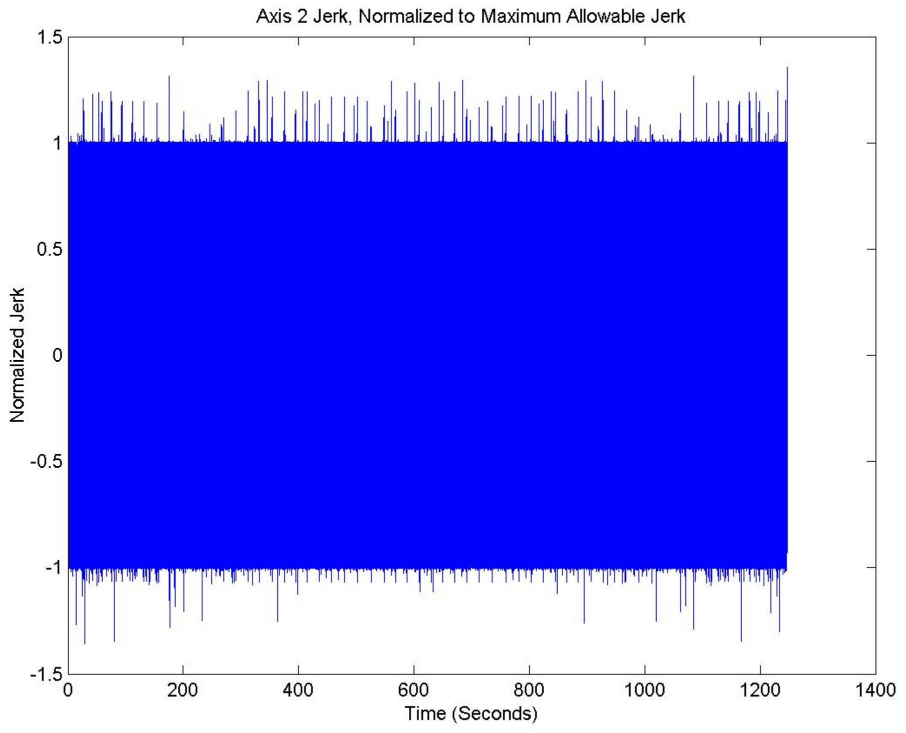

Figure 6.30. Dynamic jerk plot for Y axis.

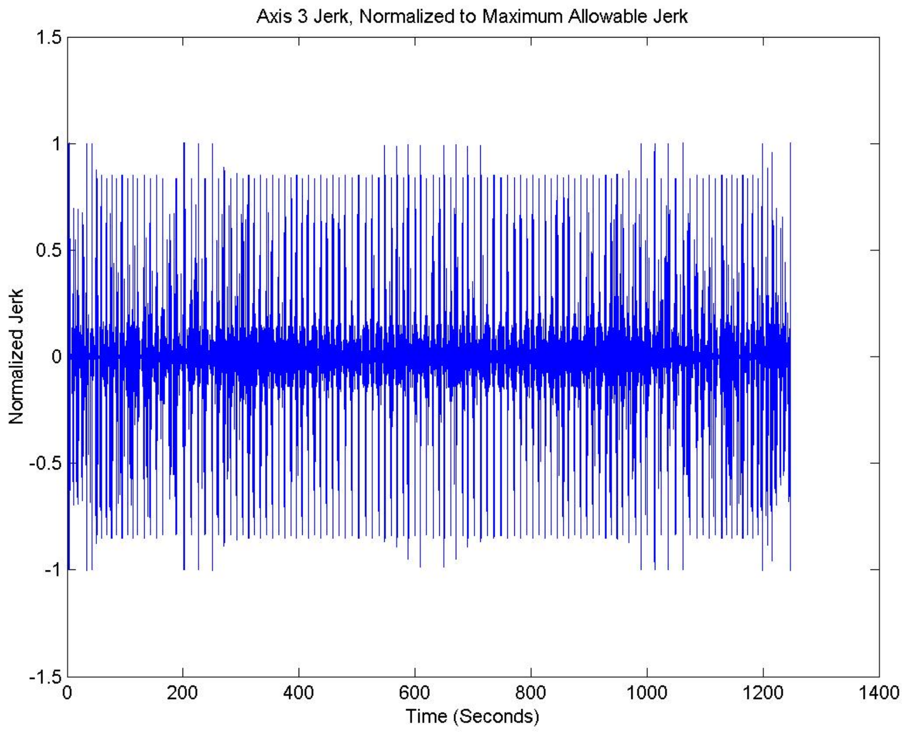

Figure 6.31. Dynamic jerk plot for Z axis.

6.2.3.5 ANALYSIS OF DYNAMICS

All the dynamic plots show joint dynamics kept within limits except for the Axis 2 jerk plot (Fig. 6.30), which shows intermittent jerk violations of up to 40%.

Some of these high jerk values are caused by the transition from one NURBS curve to another, where the ends of the curves are not curvature continuous. The smoothing of such transitions is beyond the scope of this thesis. Removing the steps that include such transitions yields a better picture of the performance of the algorithms in this thesis and gives the plot in Fig. 6.32. This plot shows improved results, with most violations at around 10%, with occasional violations up to 25%. While there is room for improvement, violations of this magnitude are of little concern. Jerk is extremely sensitive to any perturbation, and disruptions of smooth motion typically show up as jerk violations of several orders of magnitude.

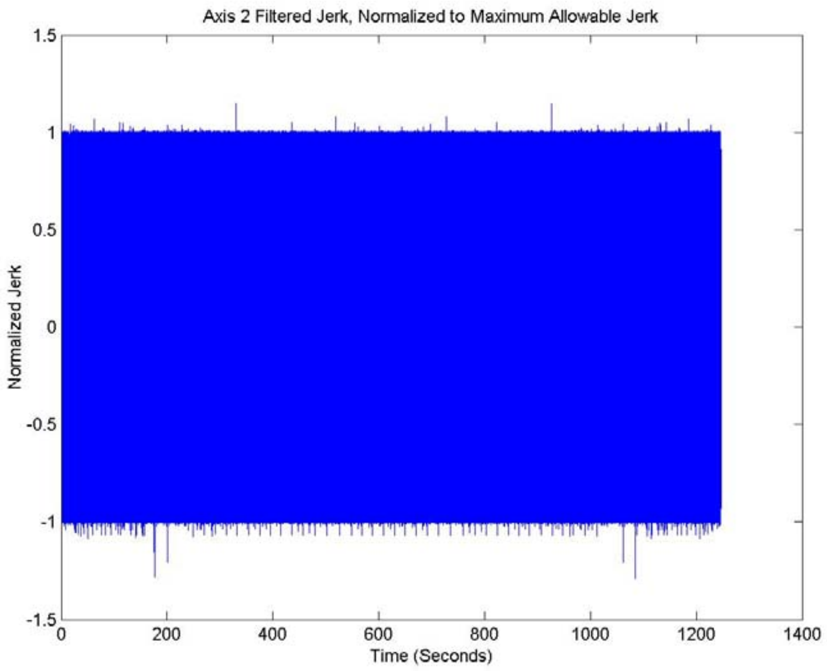

Figure 6.32. Dynamic jerk plot for Y axis, transitions removed.

6.3 MACHINED PART

Fig. 6.33 shows the automotive surface as machined. Visual inspection of the surface indicates that the part was machined correctly and yields results comparable to traditional machining methods.

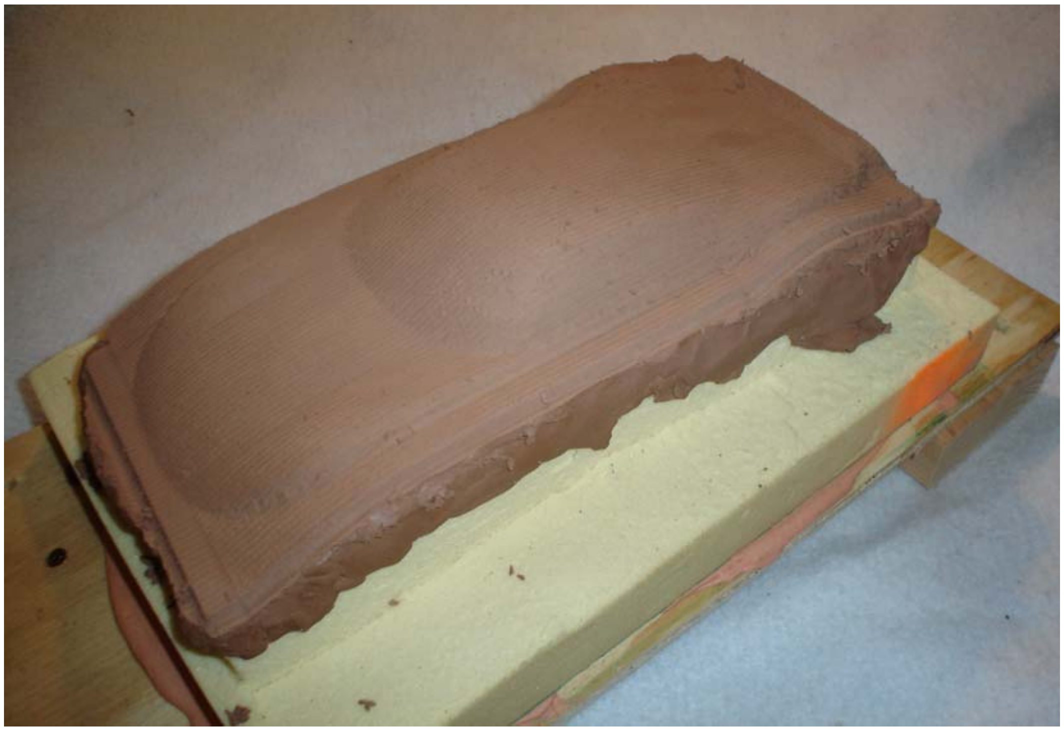

Figure 6.33. Machined automotive surface.

6.4 RESULTS SYNOPSIS

The clay part was machined correctly. Visual inspection confirms the shape of the CAD model was reproduced in the part. More importantly, the geometry-based motion planning concept was validated.

The three main portions of the motion planner appear to work well together. The predictor-corrector is obeying the specified feed rate error, the Motion Dynamics module correctly limits the speed, save for some minor jerk infractions, and the Speed Profiler is correctly following the limits imposed by the Motion Dynamics module.

7 CONCLUSION AND RECOMMENDATIONS

This thesis has developed a working geometry-based parametric curve module for the DMAC controller's motion planner. This module allows for motion over parametric polynomial curves such as Bezier and NURBS curves. The actual geometry provided by the process planning software was used, providing for a parametric curve module that is completely geometry-based. The four important aspects of motion: feed rate error, path accuracy, motion dynamics, and speed profiling were successfully integrated into a motion planning module and tested on a real-world part surface.

A stable predictor-corrector was developed, allowing for accurate specification of the feed rate error to 0.0001%. An approach to motion dynamics and path accuracy was developed that keeps the speed, acceleration, and jerk of machine axes and the chordal machining error within set limits. A stable, reliable two-pass speed profiler was developed that maintains controlled motion and tool speed with minimal calculation time.

These methods were tested on an automotive body panel, machined in a clay medium on BYU's Tarus styling mill. The results from this test verified that the methods proposed and implemented are working and fulfill the goals of this thesis.

7.1 FUTURE WORK

This thesis opens up a new area of research within machine control. That is, controlling a machine by directly following parametric geometry, without pre-tessellation. Suggestions for further research, including improvements and extensions to these methods, are listed below.

- Optimize the speed profiler to allow more time at or near the desired speed. The speed profiling algorithm in this thesis requires that the path acceleration be zero at the endpoints of each curve segment. Better response from the machine can be attained if this requirement can be eliminated. Additionally, the current speed profiling algorithms specify the worst-case allowable speed, acceleration, and jerk values for an entire curve segment. Integrating methods, such as that of Timar et al. [31], that account for the continuous variation of these values will yield additional gains.

- The speed and dynamic response of the machine tool is limited by the interplay between the tool path curve geometry and the kinematics of the machine tool. Developing and applying methods that morph the curve to be more compliant to the kinematics of the machine tool will allow for better path speeds and response. These methods must respect the manufacturing tolerance.

- Typical servo control algorithms operate on a point-to-point methodology. Integration of the curve definition with the servo control algorithms may yield some benefits.

- Extension of methods to include orientation control will allow for geometry-based 5-axis machining.

- Comparisons of geometry-based methods to tessellated methods will give researchers and industry an understanding of the benefits and limitations of geometry-based methods. Suggestions for such research include comparisons of processor requirements, suitability for different kinematic configurations, attainable path speeds, accuracy, and data management/product lifecycle impacts.

8 REFERENCES

1. Bassett CP, Jensen CG, Bosley JE, Red WE, Evans MS. Direct Machining: A New Paradigm Machining Data Transfer. 5th Design for Manufacture Conference - ASME 2000 Design Engineering Technical Conferences. Baltimore, MD. paper no. DFM-1498. Sept. 10-13, 2000.

2. Bemporad A, Tarn TJ, Xi N. Predictive Path Parameterization for Constrained Robot Control. IEEE Transactions on Control Systems Technology. 1999. v7. n6. p648-656.

3. Cheatham RM, Red WE, Jensen CG. Direct Process Control Using n-Dimensional NURBS Curves. Computer Aided Design and Applications 2005. v2. n6. p825-834.

4. Cheatham RM, Red WE, Jensen CG. n-Dimensional NURBS for Direct Control of Mechanisms. Japan-USA Symposium on Flexible Automation. July 19-21, 2004. Denver, Colorado, USA.

5. Cheng MY, Tsai MC, Kuo JC. Real-time NURBS Command Generators for CNC Servo Controllers. International Journal of Machine Tool and Manufacture. 2002. v42. p801-813.

6. Chou JJ, Yang DCH. Command Generation for Three-Axis CNC Machining. Journal of Engineering for Industry. 1991. v113. p305-310.

7. Dong J, Stori JA. Optimal Feed-Rate Scheduling for High Speed Contouring. ASME International Mechanical Engineering Congress. Washington, D.C. November 15-21, 2003. p497-513.

8. Erkorkmaz K, Altintas Y. High Speed CNC System Design. Part I: Jerk Limited Trajectory Generation and Quintic Spline Interpolation. International Journal of Machine Tools and Manufacture. 2001. v41. p1323-1345.

9. Farin G. Curves and Surfaces for CAGD, 5ed. Morgan Kaufmann. 2002.

10. Farouki RT, Sakkalis T. Real Rational Curves are not 'unit speed.' CAGD. 1991. v8. p151-157.

11. Farouki RT, Shah S. Real-Time CNC Interpolators for Pythagorean Hodograph Curves. CAGD. 1996. v13. p583-600.

12. Günter B, Parent R. Computing the Arc Length of Parametric Curves. IEEE Computer Graphics and Applications. 1990. p72-78.

13. Horsch T, Jüttler B. Cartesian Spline Interpolation for Industrial Robots. CAD. 1998. v30. n3. p217-224.

14. Jüttler B, Wagner MG. Computer-aided design with spatial rational B-spline motions. ASME Journal of Mechanical Design. 1996. v118. n2. p193-201.

15. Jüttler B, Wagner MG. Rational Motion-Based Surface Generation. CAD. 1999. v31. p203-213.

16. Kim JH, Ruyh BS, Pennock GR. Development of a Trajectory Generation Method for a Five-Axis NC Machine. Mechanism and Machine Theory. 2001. v36. p983-996.

17. Koren, Yoram. Computer Control Of Manufacturing Systems. McGraw-Hill. 1983.

18. Koren Y, Masory O. Reference-Pulses Circular Interpolators For CNC Systems. Journal of Engineering for Industry. 1981. v103. n1. p131-136.

19. Kythe PK, Schaeferkotter MR. Handbook of Computational Methods for Integration. Chapman & Hall/CRC Press. 2005.

20. Li W, Davis T, Jensen CG, Red WE. Rapid and flexible prototyping through direct CNC. Computer-Aided Design and Applications. v1. n1-4. p91-100. 2004.

21. Liu X, Ahmad F, Yamazaki K, Mori M. Adaptive Interpolation Scheme for NURBS Curves with the Integration of Machining Dynamics. International Journal of Machine Tools and Manufacture. 2005. v45. p433-444.

22. Nam SH, Yang MY. A Study on a Generalized Parametric Interpolator with Real-Time Jerk-Limited Acceleration. CAD. 2004. v36. p27-36.

23. Piegl L, Tiller W. The NURBS Book, 2ed. Springer Verlag. 1997.

24. Red EW. A Dynamic Optimal Trajectory Generator for Cartesian Path Following. Robotica. 2000. v18. p451-458.

25. Renton D, Elbestawi MA. High Speed Servo Control of Multi-Axis Machine Tools. International Journal of Machine Tools and Manufacture. 2000. v40. p539-559.

26. Reintjes, J Francis. Numerical Control Making A New Technology. Oxford University Press. 1991.

27. Sarfraz M. A Rational Cubic Spline for the Visualization of Monotonic Data. Computers and Graphics. 2000. v24. p509-516.

28. Sarma R, Rao A. Discretizors and Interpolators for Five-Axis CNC Machines. Journal of Manufacturing Science and Engineering. 2000. v122. p191-197.

29. Shoemake K. Animating Rotation with Quaternion Curves. ACM Siggraph. 1985. v19. n3. p245-254.

30. Shpitalni M, Koren Y, Lo CC. Realtime Curve Interpolators. CAD. 1994. v26. n11. p832-838.

31. Timar SD, Farouki RT, Smith TS, Boyadjieff CL. Algorithms for Time-Optimal Control of CNC Machines Along Curved Tool Paths. Robotics and Computer-Integrated Manufacturing. 2005. v21. p37-53.

32. Tsai MC, Cheng CW. A Real-Time Predictor-Corrector Interpolator for CNC Machining. Journal of Manufacturing Science and Engineering. 2003. v125. p449-460.

33. Wagner MG. Planar rational B-spline motions. CAD. 1995. v27. n2. p129-137.

34. Wagner MG, Pottmann H. Geometric Motion Design. in Modelling and Planning for Sensor-Based Intelligent Robot Systems, Series in Machine Perception and Artificial Intelligence. v21. World Scientific. 1995. p104-119.

35. Wang FC, Yang DCH. Nearly Arc-Length Parameterized Quintic Spline Interpolation for Precision Machining. CAD. 1992. v25. p281-288.

36. Yang DCH, Chou JJ. Automatic Generation of Piecewise Constant Speed Motion with Smooth Transition for Multi-Axis Machines. Journal of Mechanical Design. 1994. v116. p581-593.

37. Yang DCH, Kong T. Parametric Interpolator Versus Linear Interpolator for Precision CNC Machining. CAD. 1994. v26. n3. p225-234.

38. Yang Z, Red WE. On-line Cartesian Trajectory Control of Mechanisms Along Complex Curves. Robotica. 1997. v15. p263-274.

39. Yeh SS, Hsu PL. The Speed-Controlled Interpolator for Machining Parametric Curves. Computer-Aided Design. 1999. v31. p349-357.

40. Yeh SS, Hsu PL. Adaptive-feedrate Interpolation for Parametric Curves with a Confined Chord Error. CAD. 2002. v34. p229-237.

41. Yong T, Narayanaswami R. A Parametric Interpolator with Confined Chord Errors, Acceleration and Deceleration for NC Machining. CAD. 2003. v35. p1249-1259.

42. Zhang QG, Greenway RB. Development and Implementation of a NURBS Curve Motion Interpolator. Robotics and Computer-Integrated Manufacturing. 1998. v14. p27-36.